POLITECNICO DI TORINO

III Faculty of Engineering

Electronic Engineering

Master Degree Thesis

High efficiency high step-down DC-DC conversion- the Ćuk-Buck 1.5 converter

Supervisors:

Prof. Franco Maddaleno

Prof. Keyue Smedley

Candidate:

Ermanno Citraro

Contents

I INTRODUCTION

High efficiency power conversion research aims either to mitigate PWM hard switching and magnetic leakage losses or to discover new topologies inherently free of these issues. Following the first direction resonant switches have been obtained in [1]. However, being applied to the well-known PWM converters, they change and complicate the input-output conversion ratio $M = \frac{VO}{VG}$. In [2,4] passive and active fixing cells do not change the PWM's M but the complexity of the circuit increases. In general, this approach can improve efficiency but the number of components increases so that, if not carefully designed, the adjusted circuit results in larger overall losses. Non-PWM circuits are more attractive for the highlighted goal.

The family of resonant converters [5] naturally achieves ZVS on its switches but conversion ratio and voltage regulation capability via frequency modulation strongly depend on the load; moreover, high rms currents circulate in the circuit increasing conduction loss. The Ćuk-Buck converter [6] comes instead from the switched-capacitor family; by means of added resonant inductors it solves the main problems that afflict this category i.e. fixed conversion ratio and high current spikes. Ćuk's circuit allows very high efficiency by avoiding inductive energy storage (in the form of DC current) and by exploiting the resonant current waveform to achieve ZCS during three of the four possible active switching moments. The resonant hybridization of the otherwise 2to1 switched-capacitor circuit causes a not so important load dependency in M but benefits of fast output current transients at load changes: this is an important feature when supporting a digital circuit. Voltage regulation is achieved by fixing the off time of the input switch and varying the on time i.e. by frequency control. The main limitation is the duty ratio being constrained by design with a not so high step-down at minimum D (which is here considered being $D = 0.15$).

This introduces the second goal of this research, high step-down, to be achieved while maintaining high efficiency. Classic solutions for high step-down include cascaded PWM converters [7] and quadratic PWM converters [8]. Cascading stages results in an overall efficiency η which decreases fast with the number of stages; with m stages $\eta = \eta_1 \cdot \eta_2 \cdot \ldots \cdot \eta_m$. Moreover, even if the energy storing magnetics can share the same core, the increasing number of components affects the reliability of the converter. On the other hand, quadratic PWM converters, which are a clever extension of cascaded PWM stages, reach high step-down with moderate duty cycles ($M = D^2$ for the Quadratic Buck) but use only one active switch. Still the efficiency is not very high due the hard switching inherited by the PWM family.

A new variable may be introduced along with D to enhance the step-down ratio. In [9] $m \triangleq \frac{N1}{N2}$ is adopted, being the winding ratio of a tapped-inductor used in place of the classic Buck inductor. For the

same D the conversion ratio M(D, m) highly decreases but the non-perfect coupling between primary and secondary causes large voltage spikes at one end of the switch compromising its life besides the efficiency of the converter. In order to protect the switch a snubber is needed but the energy stored by the leakage inductance is lost unless an energy recovering cell is designed as in the approach of [2-4].

The leakage problem of the tapped-inductor is solved by Ćuk in [10] with the Ćuk-Buck 2 being a mix of his previous Ćuk-Buck converter [6] and, indeed, the tapped-inductor Buck converter: energy is now stored in the circuit both in the capacitive and inductive form. The focus is on the well management of the coupled inductors' leakages which become functional part of the energy transfer mechanism. Moreover, only one diode is needed and both the input and output switches may achieve ZVS resulting in an optimized load independent fast transient high step-down circuit. This converter can easily perform the 48V to <12V direct conversion needed by the most recent server racks such as those of the Open Computer Project.

The present work starts from highlighting the less precise M control of the Ćuk-Buck 2 and presents a solution which brings back the fixed off time of the Ćuk-Buck, resulting in a slightly more complex circuit which takes the best of the two patents [6], [10].

II DERIVATION OF THE PROPOSED CIRCUIT

The Ćuk-Buck Converter

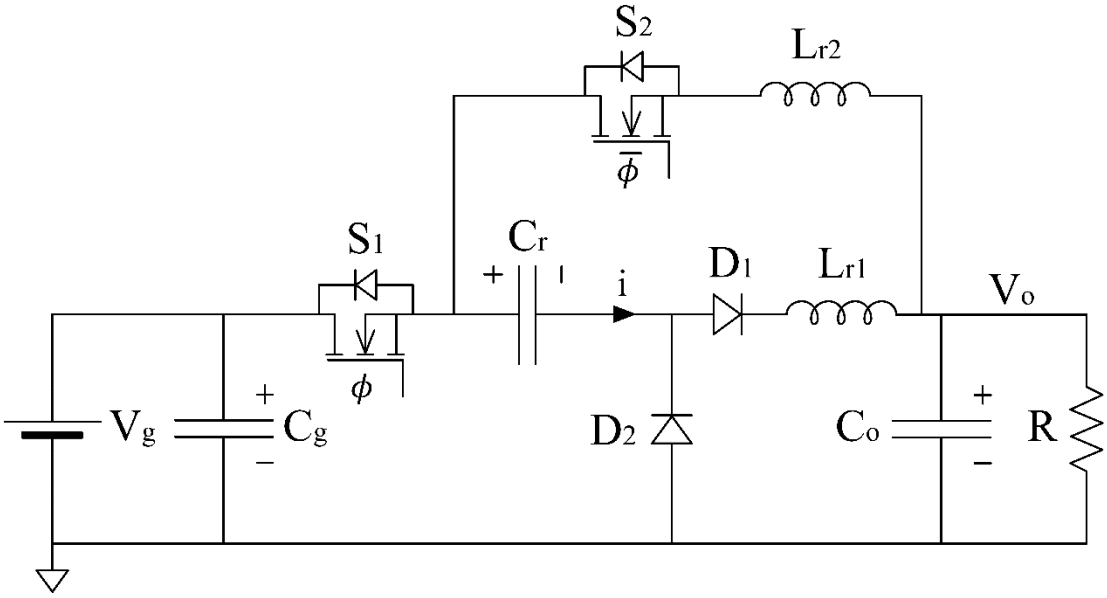

Figure 1

Fig. 1 pictures Ćuk's 2012 patent [6] and Fig. 2, 3 show its on, off circuits. Unless explicitly noted, in all following analyses the output node is considered at fixed voltage $Vo = VO$ (Co big enough).

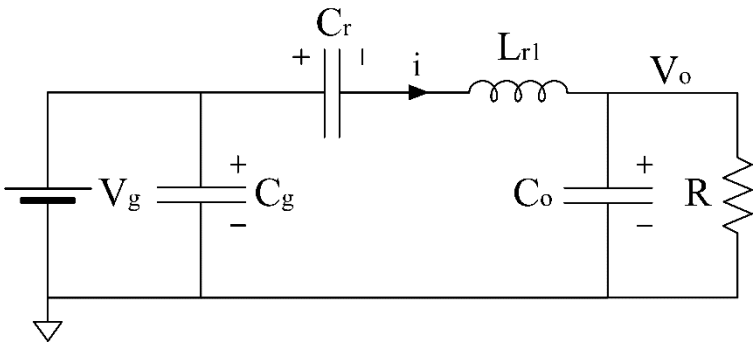

Figure 2

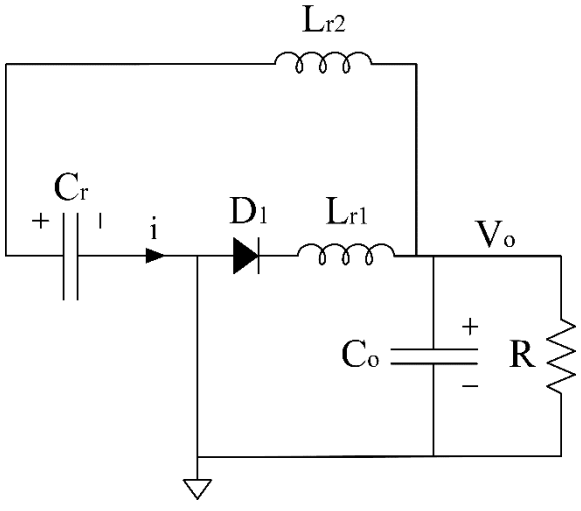

Figure 3

During the on-phase ($\phi = 1$, S1 on, S2 off) Cr charges through the Cr-Lr1 resonance started by voltage ripple $Vrp = VG - (Vcr + VO) > 0V$ since Cr was (little) discharged by R in the previous phase. In

order to get voltage regulation, the resonance stops at $\mathrm{Ton} < \pi\sqrt{\mathrm{Lr1\ Cr}} = \frac{\mathrm{Tres}}{2} = \mathrm{Ton}_{\max}$; not doing so, with $\mathrm{Ton} \geq \pi\sqrt{\mathrm{Lr1\ Cr}}$, would fix $\mathrm{M} = 0.5$ since D1 would interrupt negative current in any case for $\mathrm{t} \geq \pi\sqrt{\mathrm{Lr1\ Cr}}$ and thus the input current in Ton then delivered in Toff would be always the same independently on D with $\mathrm{IO} = 2\mathrm{IG}$.

Toff ($\phi = 0$, S1 off, S2 on) is instead fixed at $\mathrm{Toff} = \pi\sqrt{\mathrm{Lr2\ Cr}}$: during this time interval the resonant capacitor Cr releases the charged stored during Ton and Lr1 linearly discharge through D2, D1 until negative current is blocked by D1 which turns off before Toff ends[1]. As shown in Fig. 4, at $\mathrm{t} = \mathrm{DT}$, since Lr1 current can't flow through Lr2, $\mathrm{iCr} = \mathrm{i}$ drops to 0A, becomes negative through Lr2-Cr resonance and it's finally blocked at 0A by D2 while iLr1 discharges linearly from $\mathrm{iLr1(DT)} = \mathrm{i(DT^-)}$ to 0A.

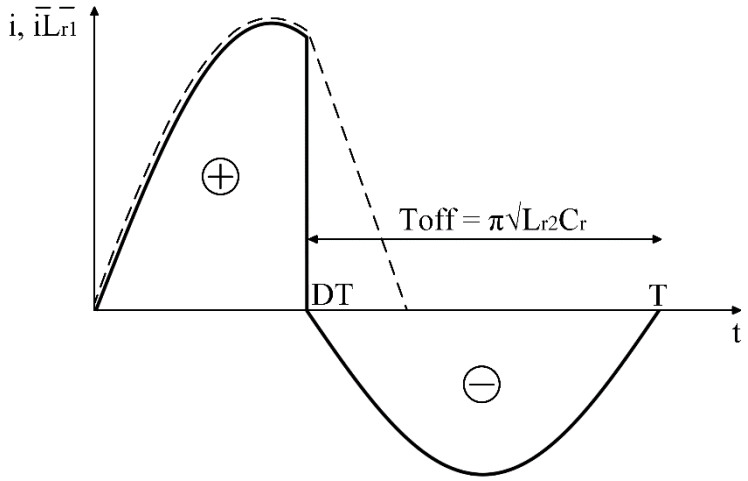

Figure 4

It follows that $\mathrm{M} = \frac{\mathrm{IG}}{\mathrm{IO}}$ is controlled by varying $\mathrm{Ton} = \mathrm{DT}$ with fixed Toff i.e. by frequency control of the switches S1, S2. It results (see [6]) $\mathrm{M} \approx \frac{\mathrm{D}}{2\mathrm{D}+\mathrm{D}_2}$ with $\mathrm{D}_2\mathrm{T}$ being the duration of the linear discharge of Lr2 in Toff. The expression of D_2 is not straightforward to get with $\mathrm{D}_2 = \mathrm{D}_2(\mathrm{D}, \mathrm{Lr1}, \mathrm{Lr2}, \mathrm{Cr}, \mathrm{T}, \mathbf{R})$: M is not load independent.

In [6] the converter is designed with $\mathrm{D}_{\max} = 0.67$: Lr1-Cr resonance lasts twice that of Lr2-Cr (symmetrical resonances are obtained with $\mathrm{D}_{\max} = 0.5$). The experimental M of a 750W 100V to 48V Ćuk-Buck converter is shown in Fig. 5:

[1] This is why diode D1 in Fig. 3 is pictured black: it means that it is both biased and un biased during Toff.

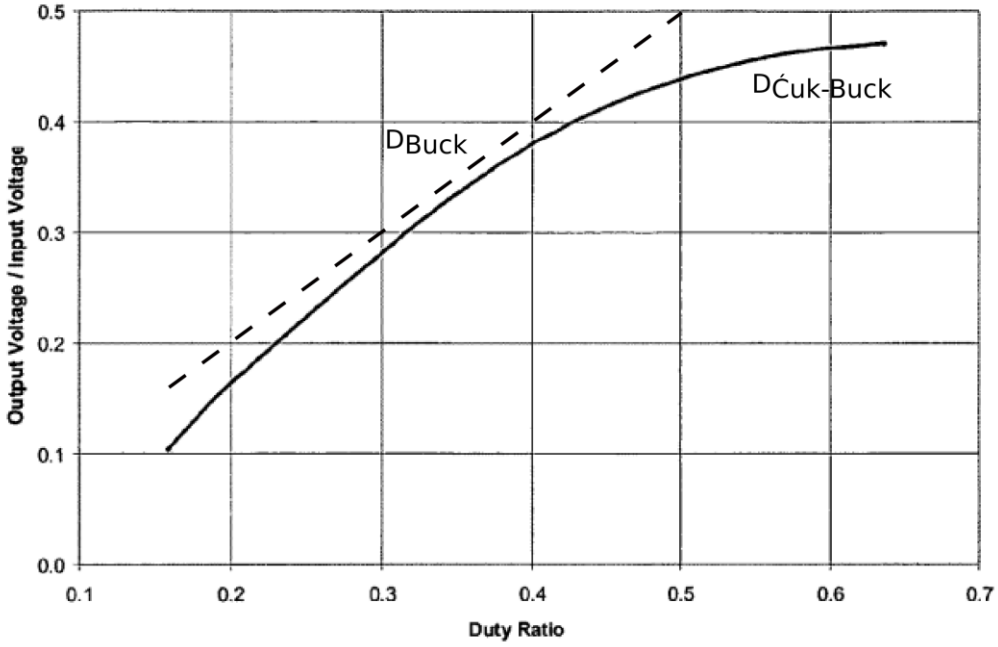

Figure 5

It is apparent that the step-down of [6] is not much greater than that of a Buck converter. Still the importance of this converter lays in its small dimensions, because of the purely resonant inductors, and in its very high efficiency (>99% for $M = 0.5$, $VO = 50V$, $PO \approx 300W$).

Towards the Ćuk-Buck 2 converter

In order to achieve higher step-down Lr1 can be transformed into an energy storing tapped-inductor; since it maintains a DC current its series diode is not needed anymore (Fig. 6);

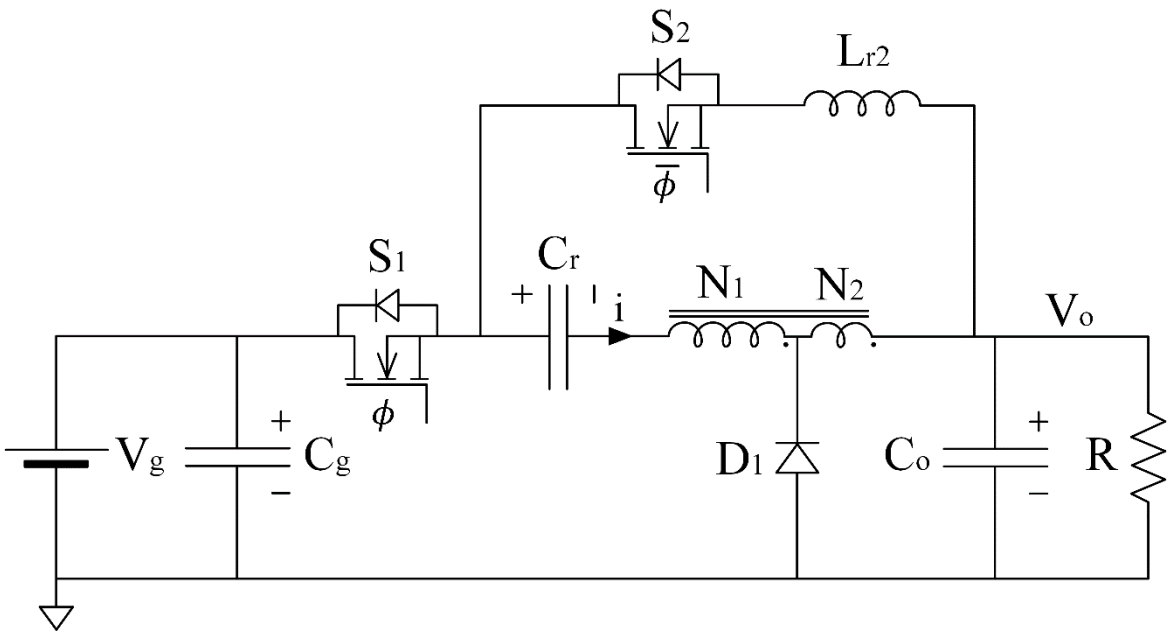

Figure 6

Knowing that during Toff $\overline{vLr2}$ = VLr2 = 0V it is:

$$VCr = VO\left(1+\frac{N1}{N2}\right) = VO\ (1+m) \tag{1}$$

Flux balance on the primary referred magnetizing inductance Lm and (1) bring

$$(VG - VCr - VO)\ \frac{N1}{N1+N2}\ D = \frac{N1}{N2} VO\ (1-D)$$

$$(VG - VO\ (1+m) - VO)\ \frac{N1}{N}\ D = m\ Vo\ (1-D)$$

from which the conversion ratio M is obtained

$$M = \frac{VO}{VG} = \frac{D\ N2}{N2\ (1+D)+N1} \tag{2}$$

Even if very high step-down can be achieved with reasonable duty ratio and winding ratio (M = 0.021 ≈ $\frac{1}{50}$ with D = 0.2 and m = 8) the circuit doesn't manage at all the leakage inductances of the coupled inductors.

During Ton the windings add together resulting in the inductor $L = Lm\frac{(N1+N2)^2}{N1^2} + Llk$ where Llk is the series of primary and secondary leakages of the coupled inductors model: both L and Llk are being charged at i. At t = DT the inductors' only available discharge path is through S2 (Fig. 7) thus the resonant inductor Lr2 experiences a high di/dt causing a voltage spike across S2.

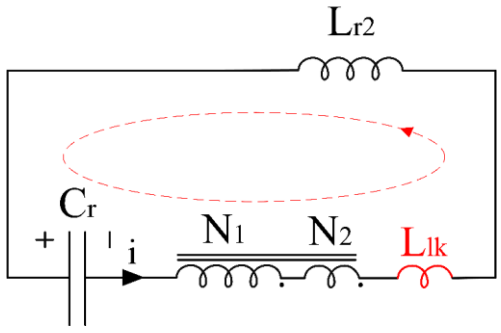

Figure 7

The Ćuk-Buck 2

The problem wouldn't occur if at t = DT Lr2 had the same current of L and Llk. This is obtained by moving Lr2 in series with Cr resulting in [10] as shown in Fig. 8a.

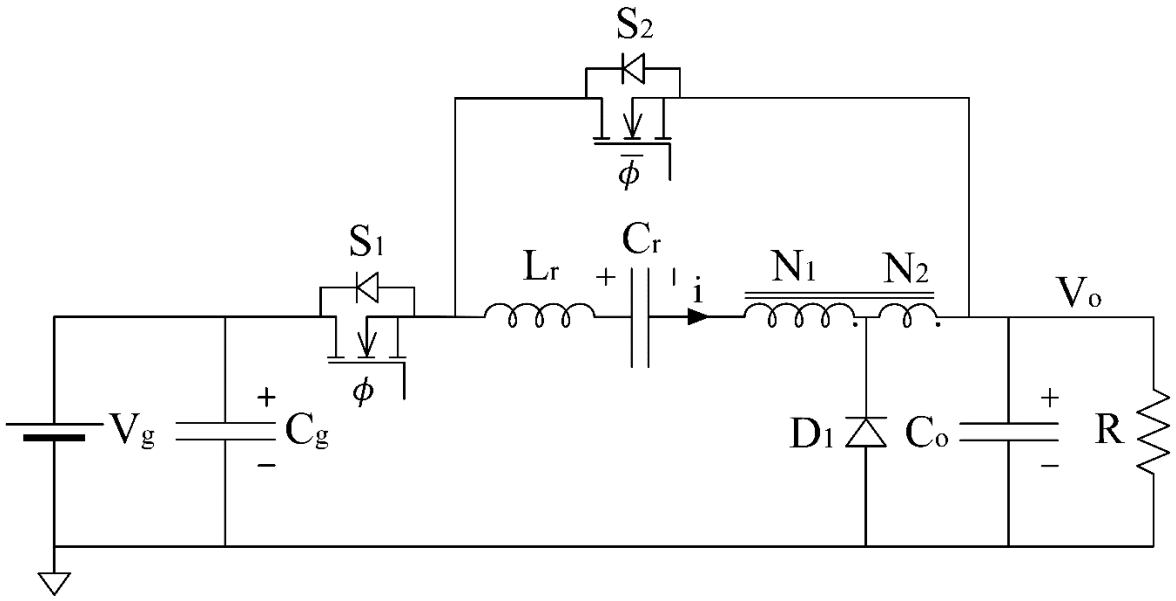

Figure 8a

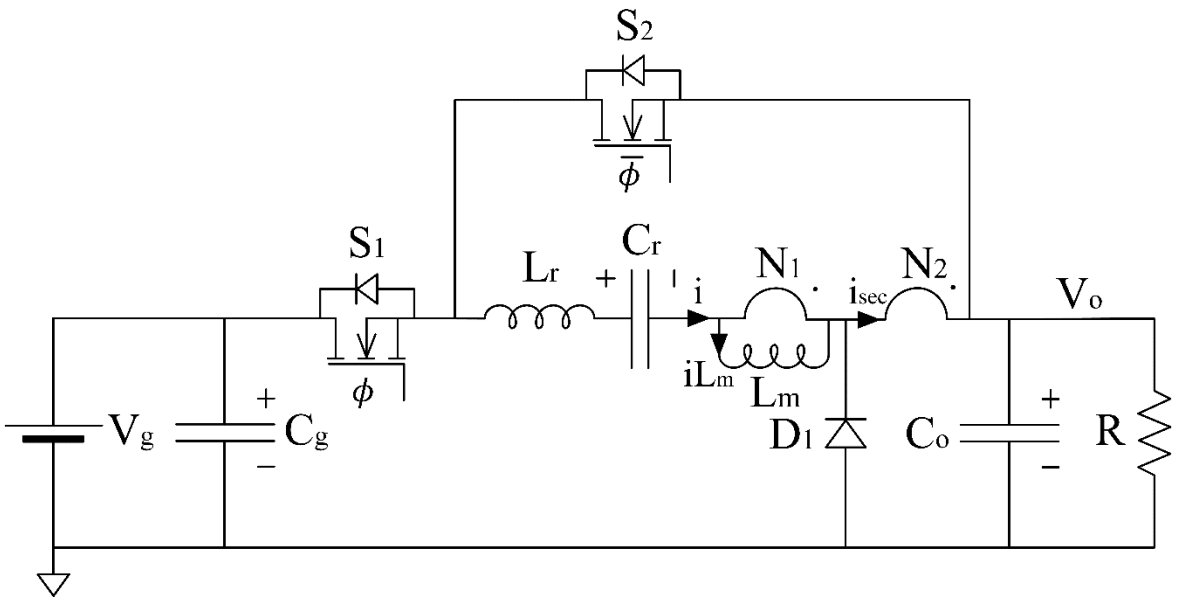

Figure 8b

Fig. 8b shows the ideal coupled inductors model which eases the understanding of the next lines. The shape of current i = iLr is shown in Fig. 9. i(0) = i(T) = 0A or equivalently Lr ends its resonance at t = T when its current tries to become positive (negative w.r.t. D1). This wanted behavior is ensured for if D1 is no more biased by iLm and thus blocks positive iLr. In general, however, iLm(T) > 0A still biases D1 and iLr can resonate negatively through it unless the period is stopped exactly at the zero crossing of the resonance. If this does not happen, iLr becomes positive during Toff and at the beginning of the next period (t > T) Lr continues charging (but with Vg) and Lm discharging through D1 until, at t = T + Γ, D1 goes off:

$$iD1 = i_{sec} - iLr = i_{sec} - \left(iLm - \frac{i_{sec}}{m}\right) = 0A \rightarrow iLm = i_{sec}\left(1 + \frac{1}{m}\right) \quad (3)$$

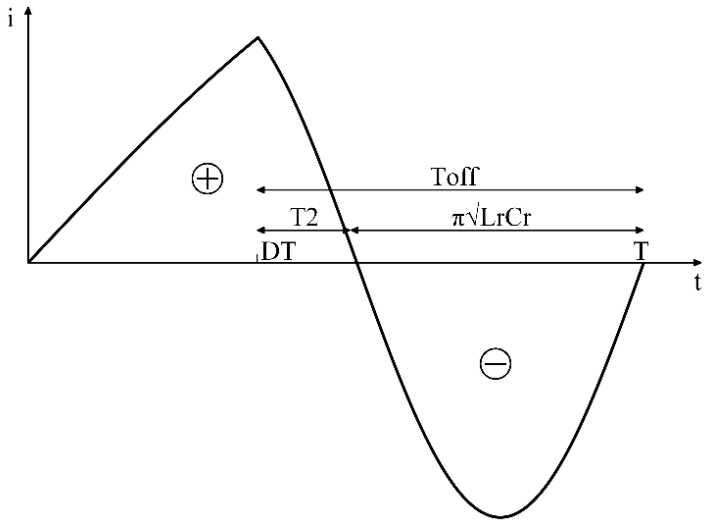

Figure 9

It follows that Toff should end when i reaches 0A with Lm ideally operating in CRitical conduction Mode (CRM)[2]: if the resonant current becomes positive before the new period starts it causes useless internal circulation since that current is being drawn from the output capacitor increasing conduction losses. A precise Toff duration is then needed but unfortunately its duration is load dependent. In fact, looking at Fig. 9, it's clear that Lr in series with L makes Cr charging during T2 after S1 is switched off so that Toff only approximately can be known and considered fixed at $\pi\sqrt{Lr\ Cr}$. At design time Toff may be decided considering the range of considered loads knowing that if R decreases i_{max} and $Toff - \pi\sqrt{Lr\ Cr} \triangleq T2$ increases.

Moreover, the presence of T2 also means that, differently from Lr2 in [6], stating $\overline{vLr} = VLr = 0V$ during Toff is an approximation since positive/negative flux is accumulated by Lr during Ton/Toff: this in turn results in an approximation of VCr and then of M in (2).

[2] If instead Lm operates in Continuous Conduction Mode (CCM), as Ton begins D1 is still biased by Lm until (3) is satisfied. No current would be drawn from the output in this case but the behavior of the circuit is not the one wanted for a short amount of time (D1 still on during Ton). There is also the possibility that during Toff iLm becomes negative through D1, biased by iLr, if Lm discharges faster than Lr and thus drawing current from the output. This should never happen in a correct design since the tapped-inductor would store little to none DC current becoming a resonant inductor itself.

The proposed circuit (Fig. 10) can achieve simultaneously the high step-down of [10] and fixed Toff of [6] resulting in a more flexible and non-parametric design. Since it mixes the two Ćuk's patents it has been called Ćuk-Buck 1.5.

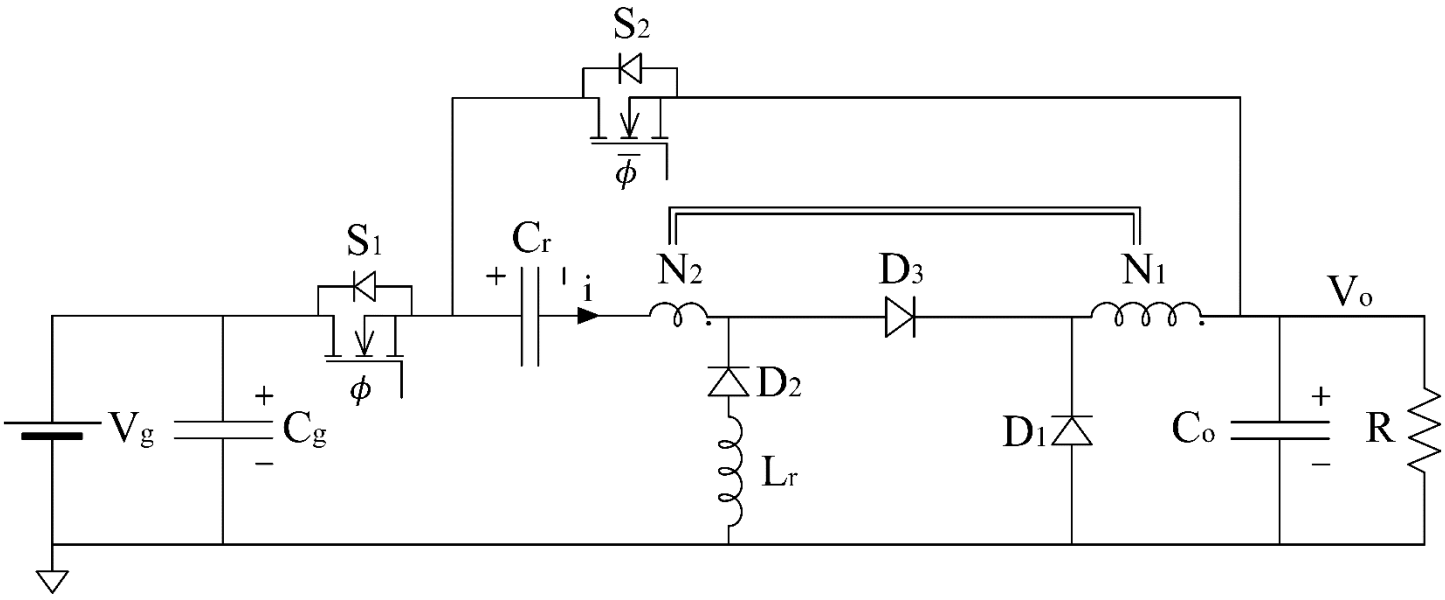

Figure 10

III ANALYSIS OF THE ĆUK-BUCK 1.5

Leakages-free analysis

First, a leakage-free analysis is performed. The on-circuit (S1 on, S2 off) is shown in Fig.11.

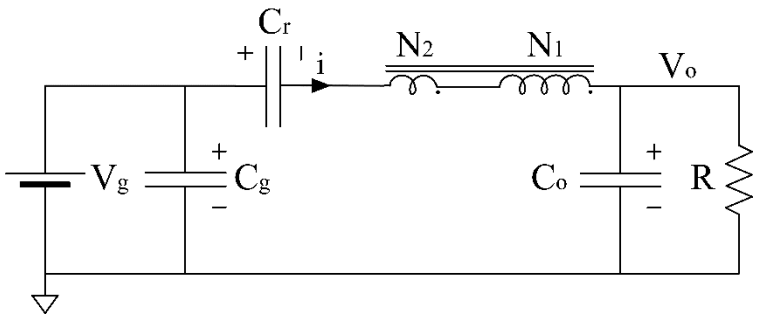

Figure 11

As in [10] Cr is charged by i through a slow quasi linear L-Cr resonant circuit with $L = Lm\frac{(N1+N2)^2}{N1^2}$, Lm being the energy storing magnetizing inductance referred to the primary side N1.

The off-circuit is shown in Fig. 12. For $t > DT$ Cr discharges through resonance with Lr whose half period $\pi\sqrt{Lr\ Cr}$ defines the duration of Toff: this is similar to [6] with Lr-Cr instead of Lr2-Cr. At the same time Lm discharges linearly to the output since VO lays across the primary winding: the same happens in [10] while in [6] this was performed by the resonant Lr1. As in [10] the resonance current which discharges Cr additionally sums to the output current through the secondary to primary contribution of the ideal transformer in the coupled inductors model.

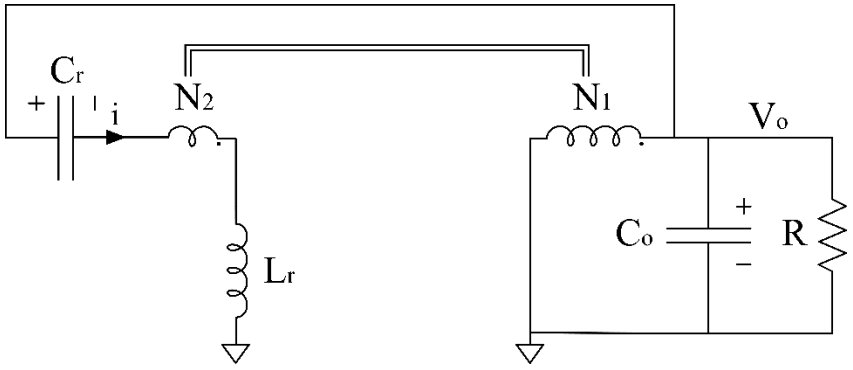

Figure 12

Overall the capacitor current shape in one period is reported in Fig. 13. It is a mix of [6] and [10]; from the latter it takes the quasi linear on-phase while from the former the fixed Toff duration.

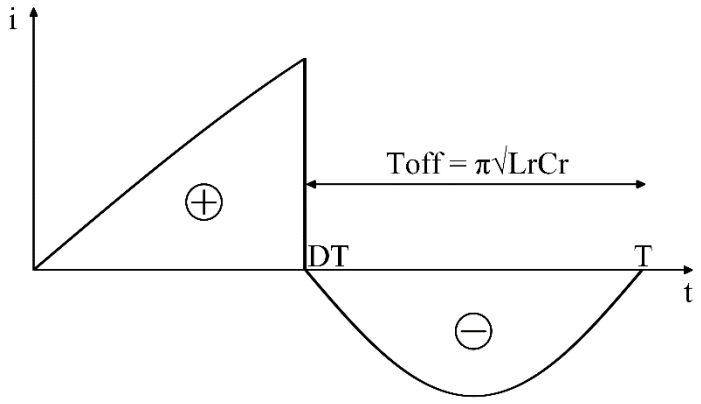

Figure 13

Differently from the Ćuk-Buck 2, it makes no difference if Lm is operating in CCM or CRM since the resonance inductor Lr is not in series with L anymore: when S1 closes D1 is for sure unbiased. Notice that the on and off circuits are the same of those in schematic Fig. 6: it follows that the conversion ratio is the same:

$$M = \frac{VO}{VG} = \frac{D\,N1}{N1\,(1+D)+N2}$$

with N2 and N1 swapped w.r.t. (2) because of author's preference ($m \triangleq \frac{N2}{N1}$).

Leakages-inclusive analysis

The addition of D3 on top of the presented topological changes is justified by the required management of magnetic leakages whose effect is investigated in the following lines.

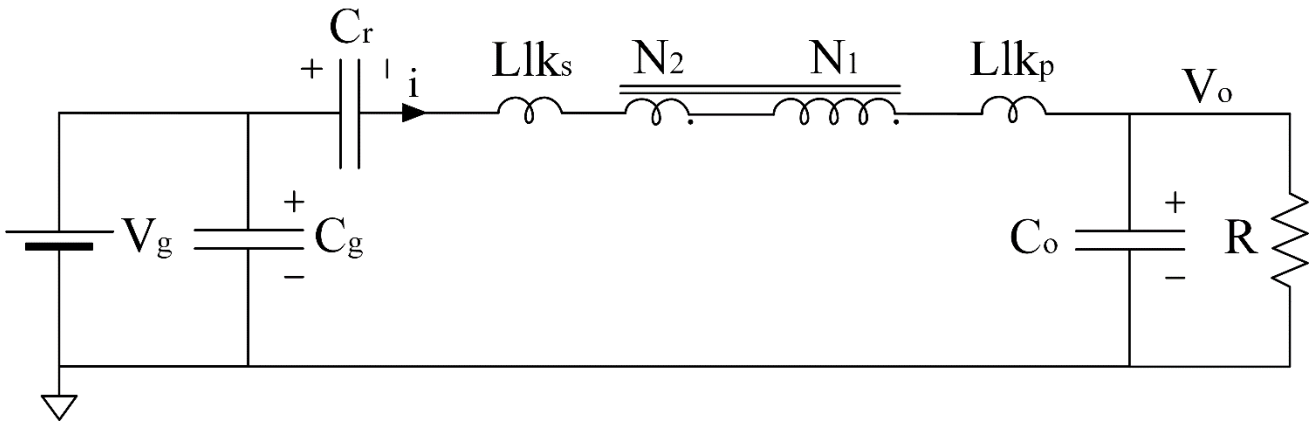

Figure 14

Fig. 14 shows the on circuit with magnetic leakages being considered at primary and secondary winding. As in [10] Llk = $Llk_p + Llk_s$ charges in series with Cr and L with the sole effect of slowing down the already long resonance.

Fig. 15 explains the function of the added D3: as S1 goes off D3 ensures Llk_p and Llk_s a discharge path through S2. As it happens in [10] the stored current in L + Llk can discharge C_{ds} of S2 and bias its body diode to let the switch turn on at zero voltage.

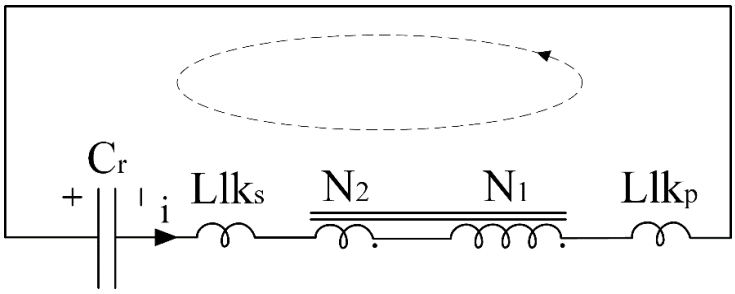

Figure 15

Notice that the circuit in Fig. 15 exists solely for few time instants after $t = DT^+$; it is in fact a fast transient during which Cr is still little charged by i and D1 turns on due to the voltage vCr being vCr > VCr.

It follows a second circuit which ends with the beginning of the Lr-Cr resonance: it is that of Fig. 16 and lasts for the time necessary to discharge the leakage Llk_s so that i reaches 0A and becomes negative.

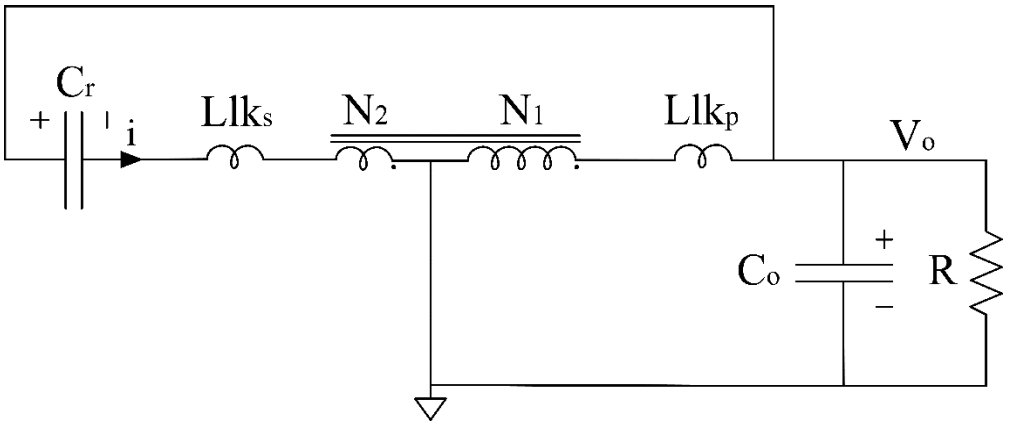

Figure 16

It's the T2 moment of Fig. 9 in [10] with the main difference that since Llk_s is small its resonant discharge with Cr is fast so that little charge coming from the output is stored in Cr which in practice can be considered fully charged at the end of Ton. In other words, T2 is here negligible because dependent on Cr-Llk_s and not on Cr-Lr resonance. This is visible in Fig. 17: after t > DT, i drops fast to 0A and it's blocked by D3 so that Cr discharges through Lr and the half resonance can start (Toff).

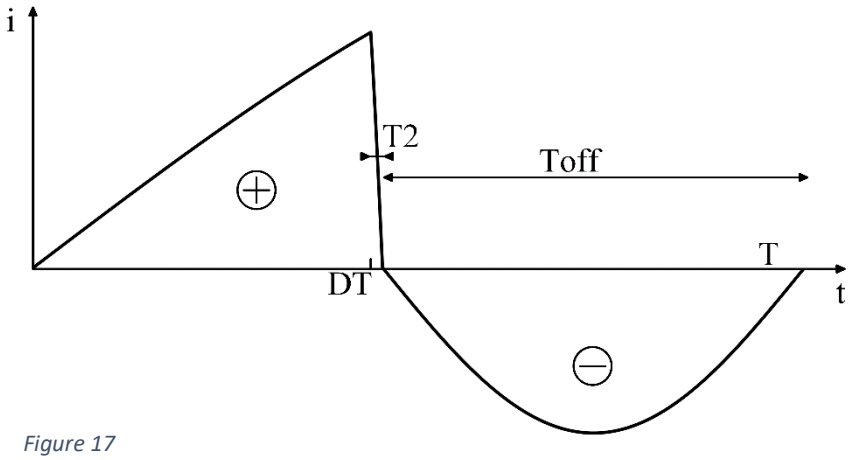

Figure 17

To sum things up, the two transitions represented by Fig. 15, 16 don't occur if leakages are not present, differently by [10] in which they always occur because of Lr.

Regarding Toff, even if Llk_s will slightly change the resonance half period from $\pi\sqrt{Lr\,Cr}$ to $\pi\sqrt{(Lr + Llks)\,Cr}$ this duration is close to the ideal fixed Toff obtained when $T2 = 0s$: the actual off-circuit is that of Fig. 18.

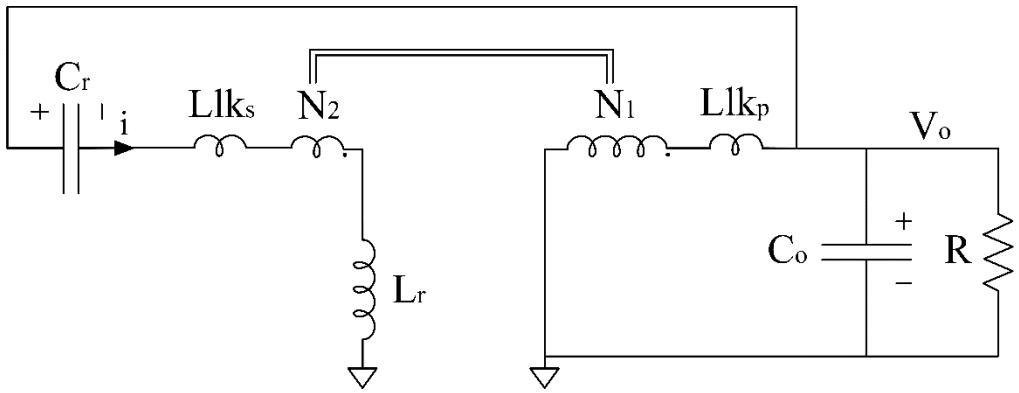

Figure 18

Since Llk_s can be considered small and so is T2, it is in good approximation

$$M = \frac{VO}{VG} = \frac{D\,N1}{N1\,(1+D)+N2} \tag{4}$$

$$Toff \approx \pi\sqrt{Lr\,Cr} \tag{5}$$

Voltage-bidirectional D3-S3

As final note, the switch 3 may be needed voltage-bidirectional to ensure the wanted behavior of the circuit; S3 may be added as shown in Fig. 19.

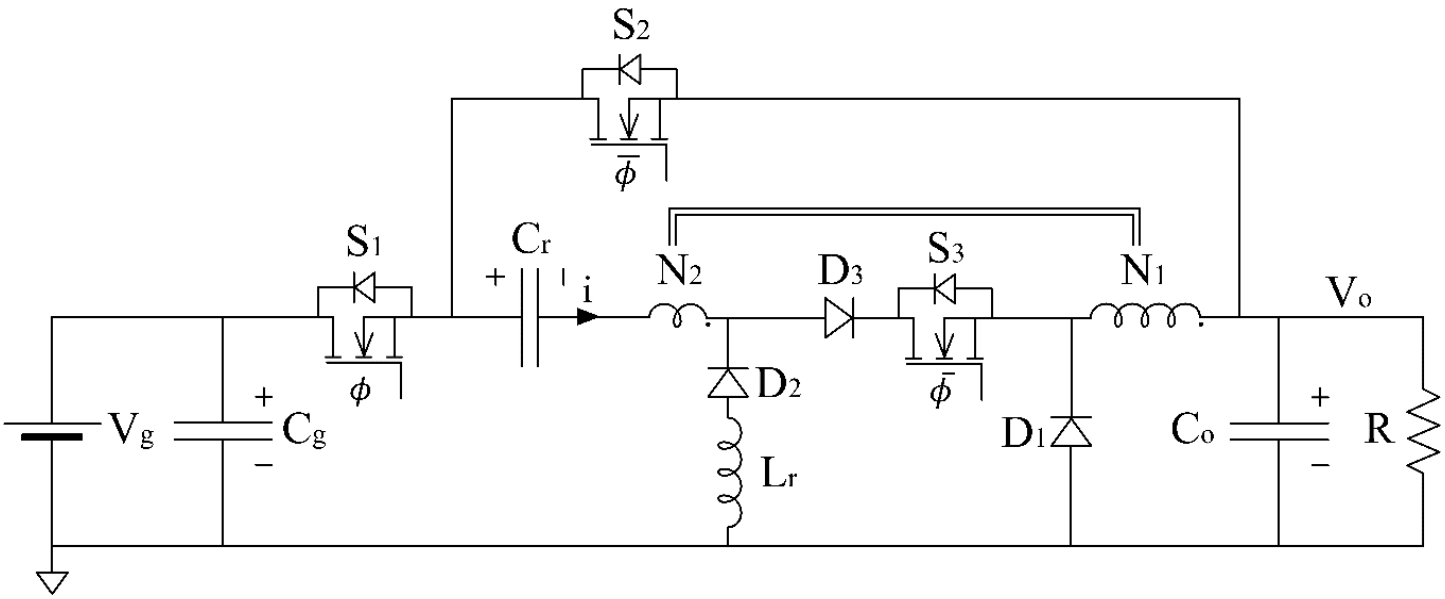

Figure 19

In fact, during Toff the current iLr = −i is sinusoidal and $vLr(t) = Lr\frac{diLr(t)}{dt}$ is cosinusoidal: after $\frac{Toff}{2} = \frac{\pi\sqrt{Lr\,Cr}}{2}$ the voltage vLr becomes negative and could bias D3: the added S3 doesn't allow any current flow if it is already off at that moment. Thus, S3 needs to be switched off at least T2 seconds after S1 and before vLr becomes negative: driving it with a delay w.r.t. S1 of $\frac{\pi\sqrt{Lr\,Cr}}{2}$ solves the problem.

In the following analysis S3 will be included but still D3 alone is sufficient under certain conditions which will be derived in chapter V.

IV WAVEFORMS AND STRESSES

The Ćuk-Buck 1.5 is shown again in Fig. 20 with the main currents oriented along the positive direction.

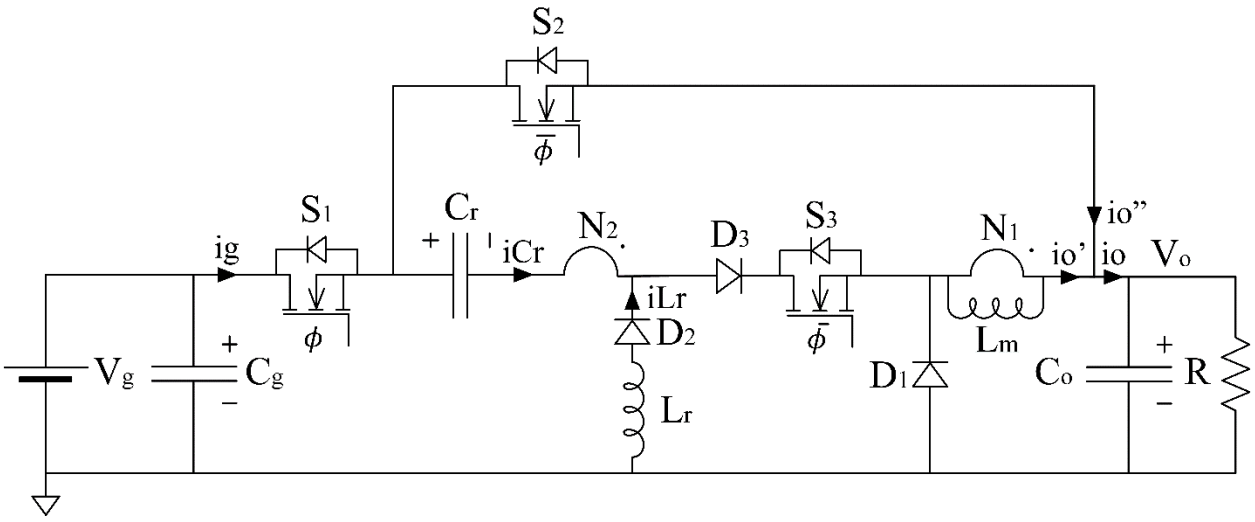

Figure 20

In the following analysis the on-phase slow resonance is approximated as linear i.e. the voltage which drops on Lm is considered constant; moreover, unless specified otherwise, diodes are treated as ideal, their forward voltage being $V_D = 0V$.

Relevant expressions

Starting from the output, the current io is sum of two contributions, a PWM-like current io_{PWM} coming from the inductance Lm during Ton and Toff (comprised in io') and a resonant current io_{res} which is eventually sum of the current generated during Toff by the Lr-Cr resonance (io'') with its primary to secondary contribution (in io'); io_{PWM}, io_{res} and io are shown in Fig. 21, 22 and 23 respectively.

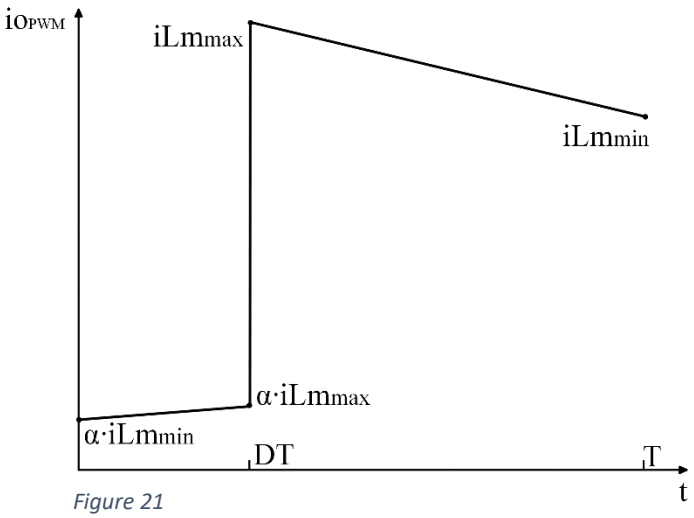

Figure 21

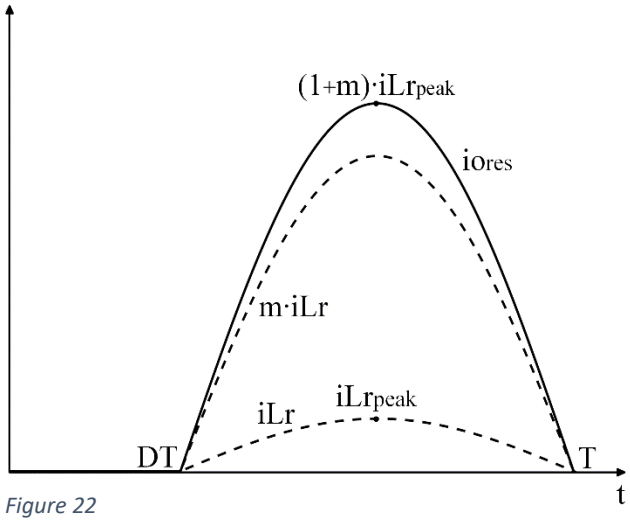

Figure 22

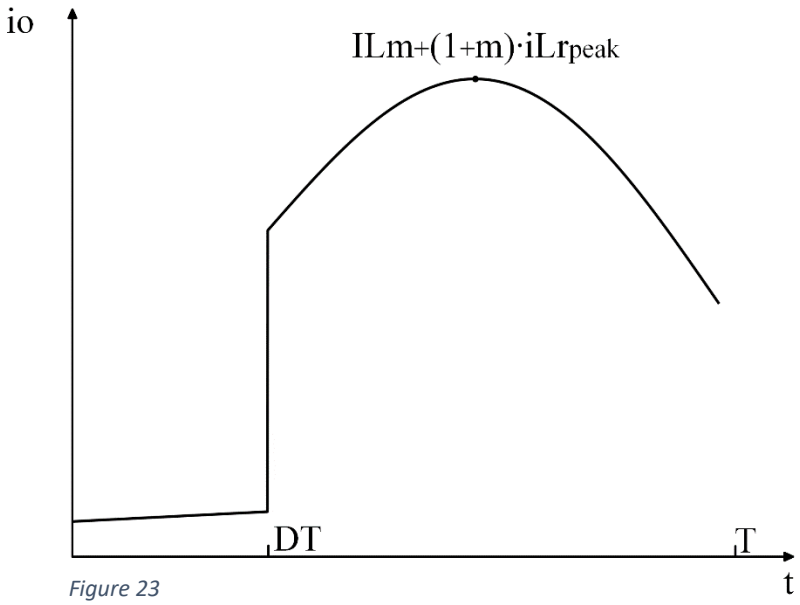

Figure 23

Knowing that the area $\int_0^{DT} \text{io}\, dt = \int_0^{DT} \text{io}_{PWM}\, dt$ represents the charge Q_g absorbed from the input and stored in Cr during Ton, it is:

$$IG = \frac{Q_g}{T} = \frac{1}{T}\int_0^{DT} io_{PWM}\, dt = \alpha(iLm_{min} + iLm_{max})\frac{D}{2} = \alpha \cdot ILm \cdot D \qquad (6)$$

with $\alpha \triangleq \frac{N1}{N1+N2} = \frac{1}{1+\frac{N2}{N1}} = \frac{1}{1+m}$.

Since the net charge accumulated by Cr over a period must be zero, Q_g coincides with the charge released by Cr during Toff i.e. $Q_g = \int_{DT}^{T} iLr\, dt$. Knowing that $Q_{o_{on}} = Q_g$, the total output charge is then

$$Q_o = Q_{o_{on}} + Q_{o_{off}} = Q_g + \int_{DT}^{T} (io_{res} + io_{PWM})\, dt = Q_g + (1+m)Q_g + Q_{Lm_{off}} \quad (7)$$

The overall charge flowing in Lm is

$$Q_{Lm} = Q_{Lm_{on}} + Q_{Lm_{off}} = (1+m)Q_g + Q_{Lm_{off}} \quad (8)$$

From (7), (8) the first important relationship is obtained:

$$Q_o = Q_g + Q_{Lm}$$

$$IO = IG + ILm \quad (9)$$

(9) tells that by increasing the step-down ratio and thus increasing IO − IG, the amount of DC current which flows in Lm increases.

The expressions of voltage ripple on Cr and current ripple in Lm are now evaluated.

$$\Delta vCr = \frac{1}{Cr}\int_0^{DT} iCr(t)dt = \frac{1}{Cr} Q_g = \frac{\alpha \cdot ILm \cdot D \cdot T}{Cr} \quad (10)$$

$$\Delta iLm = \frac{1}{Lm}\int_0^{DT} vLm(t)dt = -\frac{1}{Lm}\int_{DT}^{T} vLm(t)dt = \frac{VO}{Lm}\,(1-D)\,T \quad (11)$$

One last important quantity remains to be defined and that's the maximum resonant current iLr_{peak} during Toff. Knowing that the resonant charge under iLr equals Q_g, it is:

$$Q_g = \int_{DT}^{T} iLr(t)dt = iLr_{peak}\, T_{off}\, \frac{2}{\pi} \rightarrow IG = iLr_{peak}\,(1-D)\,\frac{2}{\pi}$$

from which

$$iLr_{peak} = \frac{IG \cdot \pi}{2(1-D)} = ILm \cdot \frac{\alpha\,\pi}{2} \cdot \frac{D}{1-D} \quad (12)$$

Knowing (6), (9), (10), (11) and (12) along with the waveforms of Fig. 21, 22 and 23, the stresses of Cr, Cg, Co, Lr, Lm, D1, D2, D3, S1, S2, S3 can be analyzed.

Stresses' equations

Cr: vCr_{max}, iCr_{rms}

$$vCr_{max} = VCr + \frac{\Delta vCr}{2} = VO(1+m) + \frac{\alpha \cdot ILm \cdot D \cdot T}{2\,Cr} \quad (13)$$

Fig. 24 shows iCr:

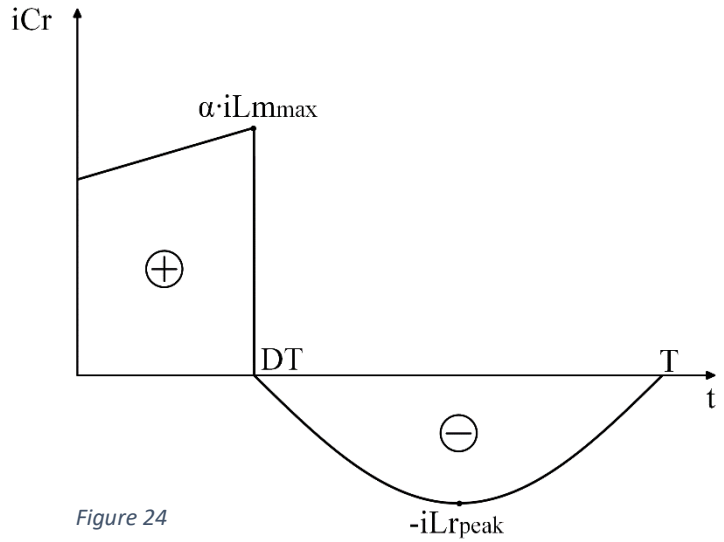

Figure 24

$$iCr_{rms}^2 = \frac{1}{T}\int_0^T \left(iCr_{on} + iCr_{off}\right)^2 dt = \frac{1}{T}\int_0^T iCr_{on}^2 + iCr_{off}^2\, dt = \frac{DT}{T}\alpha^2 \frac{iLm_{max}^2 + iLm_{min}^2}{2} +$$

$$+ \frac{1}{T}\int_{DT}^T iLr_{peak}^2 \sin(2\pi f_{res} t)^2\, dt = D\alpha^2 \frac{iLm_{max}^2 + iLm_{min}^2}{2} + \frac{iLr_{peak}^2(1-D)}{2} \approx$$

$$\approx D\alpha^2 ILm^2 + \frac{iLr_{peak}^2(1-D)}{2} = D\alpha^2 ILm^2\left(1 + \frac{D\pi^2}{8(1-D)}\right)$$

$$iCr_{rms} \approx \alpha \cdot ILm\sqrt{D\left(1 + \frac{D\pi^2}{8(1-D)}\right)} \tag{14}$$

with $f_{res} = \frac{1}{2T_{off}}$.

Cg: vCg_{work}, iCg_{rms}

$$vCg_{work} = VG \tag{15}$$

Fig. 25 shows iCg:

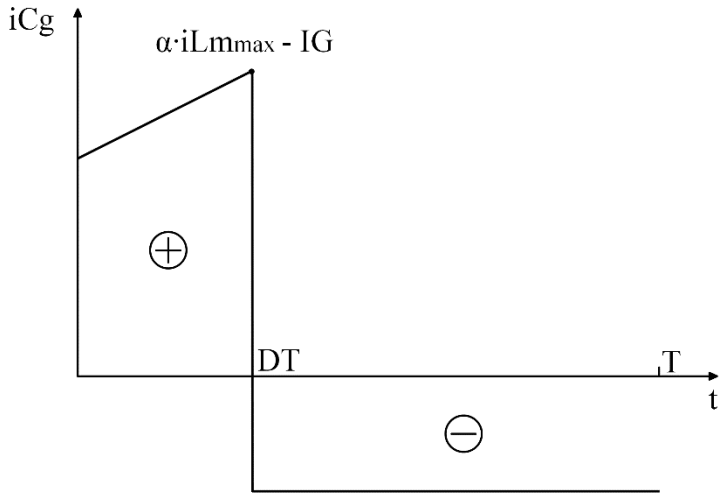

Figure 25

If Cg filters all the AC part of the current going through S1 while the input source provides its DC only, the "quadratic KCL" holds:

$$iS1_{rms}^2 = IG^2 + (-iCg_{rms})^2$$

Knowing that iS1 coincides with $io_{PWM_{on}}$, it is:

$$iS1_{rms}^2 = D\alpha^2 \frac{iLm_{max}^2 + iLm_{min}^2}{2} \approx D\alpha^2 ILm^2$$

so that

$$iCg_{rms} \approx \sqrt{D\alpha^2 ILm^2 - IG^2} \tag{16}$$

Co: vCo_{work}, iCo_{rms}

$$vCo_{work} = VO \tag{17}$$

If Co filters io_{AC} while the load current is purely IO = io_{DC}, at the output node it is:

$$io_{rms}^2 = IO^2 + iCo_{rms}^2$$

io_{rms} needs to be derived.

$$io_{rms}^2 = \frac{1}{T}\int_0^T io^2\, dt = \frac{1}{T}\int_0^{DT} io_{PWM_{on}}^2 dt + \frac{1}{T}\int_{DT}^T \left(io_{PWM_{off}} + io_{res}\right)^2 dt$$

In order to simplify calculations, the flat top approximation of the io_{PWM} is performed since now both for its on and off part:

$$io_{rms}^2 \approx \frac{1}{T}\int_0^{DT} \alpha^2 \cdot ILm^2\, dt + \frac{1}{T}\int_{DT}^{T}\left(ILm + (1+m)\cdot iLr_{peak}\sin(2\pi f_{res}t)\right)^2 dt =$$

$$= \alpha^2 \cdot ILm^2 \cdot D + \frac{8ILm\cdot iLr_{peak}(1+m)+2ILm^2\pi+iLr_{peak}^2(1+m)^2\pi}{2\pi}\cdot(1-D) \tag{18}$$

Finally,

$$iCo_{rms} = \sqrt{io_{rms}^2 - IO^2} \tag{19}$$

Lr: iLr_{max}, iLr_{rms}

Since $iLr_{on} = 0A$ and $iLr_{off} = -iCr_{off}$ (see Fig. 24), it is:

$$iLr_{max} = iLr_{peak} \tag{20}$$

$$iLr_{rms} = \sqrt{\frac{1}{T}\int_{DT}^{T} iLr_{peak}^2 \sin(2\pi f_{res}t)^2\, dt} = iLr_{peak}\sqrt{\frac{1-D}{2}} \tag{21}$$

Lm: iLm_{max}, $iPrim_{rms}$, $iSec_{rms}$

$$iLm_{max} = ILm + \frac{\Delta iLm}{2} \tag{22}$$

$$iPrim_{rms} \approx \alpha^2 \cdot ILm^2 \cdot D + \frac{8ILm\cdot iLr_{peak}\cdot m+2ILm^2\pi+iLr_{peak}^2\cdot m^2\pi}{2\pi}\cdot(1-D) \approx io_{rms} \tag{23}$$

$$iSec_{rms} = iCr_{rms} \approx \alpha \cdot ILm\sqrt{D\left(1+\frac{D\pi^2}{8(1-D)}\right)} \tag{24}$$

D1: $vD1_{rev}$, $iD1_{max}$, ID1

$$vD1_{rev} = -\frac{N2\,VO+N1(VG-vCr_{min})}{N1+N2} \tag{25}$$

$$iD1_{max} = ILm + m\cdot iLr_{peak} \tag{26}$$

$$ID1 = (1-D)\cdot ILm + m\cdot IG \tag{27}$$

D2: $vD2_{rev}$, $iD2_{max}$, ID2

$$vD2_{rev} = -\frac{N2\ VO+N1(VG-vCr_{min})}{N1+N2} = vD1_{rev} \quad (28)$$

$$iD2_{max} = iLr_{peak} \quad (29)$$

$$ID2 = IG \quad (30)$$

D3: $vD3_{rev}$, $iD3_{max}$, ID3

In order to understand vD3 and then $vD3_{rev}$, vLr is required and it is shown in Fig. 26. As Toff starts, vD3 = −vLr, D3 blocks negative voltage while the body diode of S3 is biased; this holds until vLr ≥ 0V and vD3 ≤ 0V. Then, at $t = DT + \frac{T_{off}}{2}$, vD3 can't block positive voltage while S3 does.

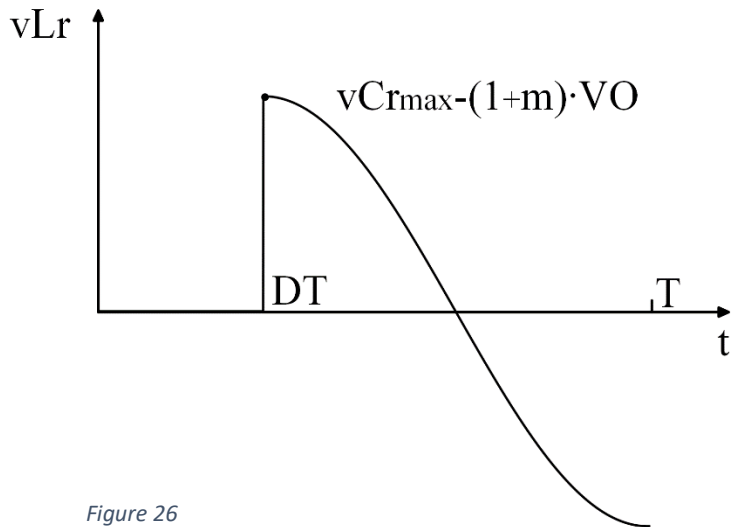

Figure 26

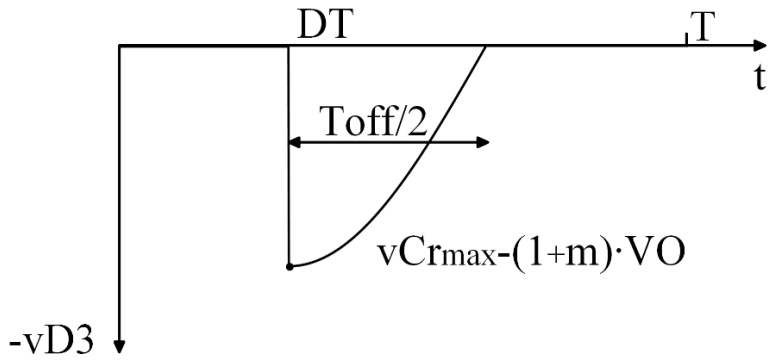

Figure 27

$$vD3_{rev} = -vCr_{max} + (1+m)\cdot VO \quad (31)$$

$$iD3_{max} = \alpha \cdot iLm_{max} = \alpha \cdot (ILm + \frac{\Delta iLm}{2}) \quad (32)$$

$$ID3 = IG \quad (33)$$

S1: $\mathrm{vds1_{max}}$, $\mathrm{is1_{max}}$, $\mathrm{is1_{rms}}$

$$vds1_{max} = VG - VO \tag{34}$$

$$is1_{max} = \alpha \cdot iLm_{max} = \alpha \cdot \left(ILm + \frac{\Delta iLm}{2}\right) = iD3_{max} \tag{35}$$

$$is1_{rms} = \alpha\sqrt{\frac{iLm_{max}^2 + iLm_{min}^2}{2} D} \approx \alpha \cdot ILm \cdot \sqrt{D} \tag{36}$$

S2: $\mathrm{vds2_{max}}$, $\mathrm{is2_{max}}$, $\mathrm{is2_{rms}}$

$$vds2_{max} = VG - VO \tag{37}$$

$$is2_{max} = iLr_{peak} \tag{38}$$

$$is2_{rms} = iLr_{peak}\sqrt{\frac{1-D}{2}} = iLr_{rms} \tag{39}$$

S3: $\mathrm{vds3_{max}}$, $\mathrm{is3_{max}}$, $\mathrm{is3_{rms}}$

In order to understand vds3 it is necessary to look at Fig. 26 and 27: when, at $t \geq DT + \frac{T_{off}}{2}$, D3 is biased by the Lr-Cr resonance, S3 blocks positive voltage across D3-S3 so that $vds3 = -vLr \geq 0V$ drops on S3.

$$vds3_{max} = vCr_{max} - (1+m) \cdot VO = -vD3_{rev} \tag{40}$$

$$is3_{max} = \alpha \cdot \left(ILm + \frac{\Delta iLm}{2}\right) = iD3_{max} \tag{41}$$

$$is3_{rms} = is1_{rms} \approx \alpha \cdot ILm \cdot \sqrt{D} \tag{42}$$

V DESIGN

Converter specifications

The chosen specifications of the dc-dc conversion are reported in Tab. 1.

VG	48 ± 2 V
VO	2 V
Δvo	≤ 5%VO = 100 mV
IO	1 to 4 A

Table 1

The nominal step down is

$$M = \frac{VO}{VG} = \frac{2}{48} = 0.0417 \quad [1]$$

Components design

Windings' turns ratio m

Fixing

$$m = \frac{N2}{N1} = 6 \quad [2]$$

in order to limit the unlinked flux of coupled inductors and solving (4) in D gives

$$D = \frac{M(1+m)}{1-M} \quad (43)$$

With [1], [2]

$$D = 0.3043 \approx 0.3 \quad [3]$$

Switching frequency f_{sw}

Since an open-loop version of the circuit is being built with no frequency control of the switches, the switching period T is chosen once for all. In order to minimize magnetic losses, hard switching loss of the input switch and to keep possible radiated waves at low frequency (EMI concerns) it is decided

$$f_{sw} = f = 70kHz \quad [4]$$

$$T_{sw} = T = 14.286\mu s$$

Maximum duty ratio D_{max}

Lr, Cr are decided according to Toff. Since T is fixed, the design must ensure that the off-phase half resonance is always completed. Lr and Cr are chosen according to $T_{off_{min}}$ which happens when $VG = VG_{min} = 46V$ so that $D = D_{max}$, $T_{on} = T_{on_{max}}$ and $T_{off} = T_{off_{min}}$. If instead T_{off} is chosen when $D = D_{min}$, $T_{off} = T_{off_{max}}$ then an increase of D for lower step-down would "erode" the off-phase length preventing the half resonance to complete. On the other hand, when $D < D_{max}$ the on-phase gets shorter and the off-phase lasts longer than the designed Lr-Cr half resonance; this is not a problem since D2 will stop it anyways. Following the above considerations, the maximum duty ratio occurs for VG_{min}:

$$M_{max} = \frac{VO}{VG_{min}} = \frac{2}{46} = 0.0435$$

$$D_{max} = \frac{M_{max}(1+m)}{1-M_{max}} = 0.3182 \approx 0.32 \qquad [5]$$

Notice that there is little difference between D_{max} and $D = D_{nom}$ because of the high step-down around $VG = 48V$. In general, if moderate conversion ratios are used, that difference widens.

Effect of diodes' forward drop on D_{max}

It is now an opportune time to consider the effect of diodes' forward voltage on conversion ratio. If [2], [3] are used VO would be smaller and, in order to compensate, D should to increase possibly above D_{max} found in [5], resulting in an interrupted Toff half resonance. Calling VD1, VD2, VD3 the nominal forward voltages of D1, D2, D3, it is (see Appendix B):

$$VO = \frac{VD1(N1(D_r-1)-N2)-D_rN1(VD2+VD3)}{N1(1+D_r)+N2} + \frac{D_rN1}{N1(1+D_r)+N2}VG \qquad (44)$$

where the term which multiplies VG coincides with M in (3). Solving for D_r gives

$$D_r = \frac{(N1+N2)(VD1+VO)}{N1(VD1-VD2-VD3+VG-VO)} \qquad (45)$$

The actual value of VD1, VD2, VD3 depends on the chosen diodes and currents flowing in them. Stresses formulas of chapter IV can be used but, while it remains true that $IG_r = IO - ILm_r$, $IG \neq M \cdot IO$. In fact, since $\frac{PO+PD}{PG} = 1$, for the same output power PO and same input voltage VG, IG increases w.r.t. previous case $\frac{PO}{PG} = 1$, where the power PD dissipated by diodes is neglected. In particular:

$$\frac{PO+PD}{PG} = \frac{IO\cdot VO+ID1\cdot VD1+ID2\cdot VD2+ID3\cdot VD3}{IG_r\cdot VG} = \frac{IO\cdot VO+((1-D)(IO-IG_r)+m\cdot IG_r)\cdot VD1+IG_r\cdot VD2+IG_r\cdot VD3}{IG_r\cdot VG} = 1 \qquad (46)$$

IG_r can be obtained once VD1, VD2, VD3 are known. Because of the circular nature of the problem, the same diodes' forward voltage is chosen as $VD = 0.4V$, IG_r and stresses are obtained, diodes are picked and their nominal VD from datasheet used to reevaluate IG_r. The stresses are updated and if the chosen diodes still suffice, those are the definitive ones.

From (43)

$$D_{r_{max}} = 0.3853 \approx 0.39 \quad [6]$$

Solving (44) for IG gives

$$IG_r = IO\,\frac{VD1(D-1)-VO}{VD1\left(D+\frac{N2}{N1}-1\right)+VD2+VD3-VG} \quad (47)$$

When $VG = 46V$, $R = 0.5\Omega$

$$IG_{r_{max}} \approx 0.21A \quad [7]$$

$$ILm_{r_{min}} = IO - IG_{r_{max}} \approx 3.79A \quad [8]$$

Without considering diodes' voltage it was $IG_{max} = IO_{max} \cdot M_{max} = IO_{max} \cdot \frac{VO}{VG_{min}} = 4 \cdot \frac{2}{46} \approx 0.17A$: diodes cause a 20% increase of the average input current. D1, D2, D3 current stresses are evaluated with [7], [8] and are reported in Tab. 2[3].

	iD_{max} [A]	**ID [A]**
D1	6.99	3.58
D2	0.53	0.21
D3	0.6	0.21

Table 2

A VSB2045Y can be used as D1 ($VD1 \approx 0.4V$ @ $ID1 \approx 3.5A$), two ZHCS400 as D2, D3 ($VD2,3 \approx 0.25V$ @ $ID1,2 \approx 0.2A$). For these forward voltages it is:

$$IG_{r_{max}} = 0.207A \approx 0.21A$$

similar to that found in [7]: there is no need to recompute the current stresses on diodes. Similarly, the maximum duty ratio doesn't change much being

[3] Current stresses are evaluated with IG_{max} and ILm_{min}; it is the worst case since using IG_{min} and ILm_{max} results in more relaxed conditions.

$$D_{r_{max}} = 0.3827$$

The maximum duty cycle is chosen as $D_{max} = \max([5], [6]) = [6] = D_{r_{max}}$: not considering the forward drop of diodes and thus picking [5] wouldn't have allowed the half resonance to complete during $T_{off_{min}}$. From now one the subscript "real" will be dropped with $D_{max} = D_{r_{max}} \approx 0.39$.

Output capacitor Co, magnetizing inductance Lm

The design can proceed with the evaluation of the minimum off-phase:

$$T_{off_{min}} = (1 - D_{max})T = 8.71\mu s = \frac{T_{res}}{2}$$

from which T_{res} and so Lr, Cr can be designed.

It was previously stated $T_{res} = 2\pi\sqrt{LrCr}$ which is indeed obtained during off-phase considering the output voltage fixed at VO or in other words considering an ideal infinite output capacitor Co. This statement is of course false and a better approximation of the resonant period is given by

$$T_{res} = 2\pi\sqrt{LrCr} \cdot \sqrt{\frac{Co}{Co + Cr(1+m)^2}} \tag{48}$$

obtained considering a finite Co but still neglecting the effects of R and Lm (see Appendix A); unfortunately, by refining the model and including also these variables, Wolfram Mathematica doesn't provide an analytical solution. From (48) Co may be chosen such that $Co \gg Cr(1+m)^2$ and $T_{res} \approx 2\pi\sqrt{LrCr}$ or the actual expression (48) can be considered without imposing such a constraint on Co. According to the type of capacitor, electrolytic or ceramic, either way can be pursuit.

In the first case, Co being an electrolytic capacitor, the voltage output ripple is decided by ESR_{Co}:

$$\Delta vo_{ele} = \Delta iCo \cdot ESR_{Co} \tag{49}$$

ΔiCo being the peak to peak current flowing in Co. Since iCo is the ac part of io (Fig. 23) its peak to peak value is

$$\Delta iCo = \Delta io = ILm + (1+m)iLr_{peak} - \alpha \cdot iLm_{min} \tag{50}$$

ESR_{Co} must be

$$ESR_{Co} \leq \frac{\Delta vo_{max}}{\Delta iCo} \tag{51}$$

Δvo_{max} being the maximum output voltage ripple from specifications. Co_{ele} can be chosen to satisfy (51) and to provide a capacitance $Co_{ele} \gg Cr(1+m)^2$. To solve (51), ΔiCo and thus iLm_{min} is needed: Lm must be designed.

Since it is a filter inductor, hysteresis losses are negligible if current ripple is small enough: $\Delta iLm_{max} = 25\%ILm$ is here used as requirement. It has to be:

$$\Delta iLm = \frac{VO+VD1}{Lm}(1-D)T \leq \Delta iLm_{max} \tag{52}$$

$$Lm \geq \frac{VO+VD1}{\Delta iLm_{max}}(1-D)T \tag{53}$$

(53) must be evaluated in the worst-case scenario, when $D = D_{min} = 0.3507$ (and $ILm = ILm_{max}$):

$$Lm \geq 23.4\mu H \tag{9a}$$

Moreover, iLm needs to be always greater than zero so that no current is drawn from the output capacitor; Lm must work in CCM or CRM:

$$iLm_{min} \geq 0A \rightarrow ILm - \frac{\Delta iLm}{2} \geq 0A \rightarrow ILm - \frac{VO+VD1}{2Lm}(1-D)T \geq 0A$$

from which

$$Lm \geq \frac{VO+VD1}{2ILm}(1-D)T \tag{54}$$

Again, with $D = D_{min}$:

$$Lm \geq 2.92\mu H \tag{9b}$$

Lm is chosen as

$$Lm \geq max([9a],[9b]) \rightarrow Lm = 25\mu H \tag{9}$$

resulting in

$$\Delta iLm_{max} = 0.89A$$

$$iLm_{max} = 4.25A$$

$$iLm_{min} = 3.36A$$

Going back to the design of the output capacitor, (50) can be maximized with $D = D_{max}$ so that $iLr_{peak} = iLr_{peak_{max}} = 0.53A$:

$$\Delta iCo_{max} = 7A$$

Then,

$$ESR_{Co} \leq \frac{100mV}{7A} = 0.0143\Omega$$

$$ESR_{Co} \approx 0.014\Omega = 14m\Omega \qquad [10a]$$

If instead a ceramic capacitor is chosen, the equality $Co \gg Cr(1+m)^2$ may be not easy to satisfy due to the lower capacitance of ceramic components. The actual resonance period (48) is considered and again Co is designed according to Δvo_{max} specification with the output voltage ripple determined now by the amount of positive/negative charge that charges/discharges Co and thus on the capacitance itself:

$$\Delta vo_{cer} = \frac{1}{Co_{cer}} \int_0^T Q_{Co}^{+}\, dt = -\frac{1}{Co_{cer}} \int_0^T Q_{Co}^{-}\, dt$$

Fig. 28 shows iCo for given loads $IO = 1, 2, 3, 4A$; considering for example $IO = 1A$ (light blue line) Δvo_{cer} can be approximated considering as Q_{Co}^{-} the green negative charge for $t < DT$, the red area being neglected. The consequent error on Δvo_{cer} is acceptable.

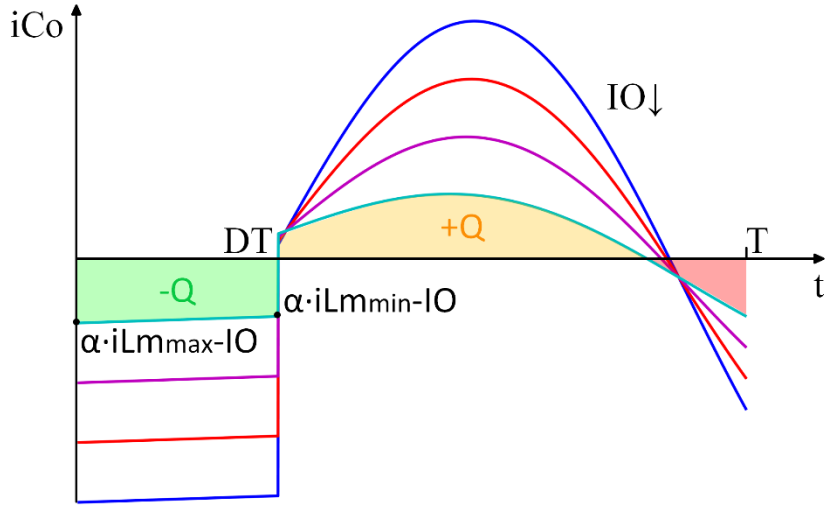

Figure 28

With this approximation it becomes:

$$\Delta vo_{cer} \approx -\frac{(\alpha \cdot ILm - IO)}{Co_{cer}} DT \leq \Delta vo_{max} \tag{55}$$

$$Co_{cer} \geq -\frac{(\alpha \cdot ILm - IO)}{\Delta vo_{max}} DT$$

With $D = D_{max}$

$$Co_{cer} \geq 189\mu F$$

Between Co_{ele} and Co_{cer} it's here preferred the second solution due to reliability concerns about electrolytic capacitors. It is chosen

$$Co_{cer} = 200\mu F \tag{10b}$$

resulting in

$$\Delta vo_{cer} = 94.5mV < 0.1V$$

Resonant capacitor Cr

Regarding Cr, its design doesn't depend on the given specifications since it's an internal resonant capacitor. Still, choosing it too small would require Lr to increase but more importantly its large voltage ripple would compromise the correct behavior of the circuit. In fact, as announced in chapter III, the aim is to have D3 alone without the need of active S3; during off-phase vD3 follows vLr which depends on ΔvCr and so on Cr. In order to correctly pick Cr, the time evolution of vD3 during Toff is needed:

$$vD3(t) = VD1 - VD2 - vLr(t) \tag{56}$$

vLr(t) analytical solution is obtainable from (A10) in Appendix A as $vLr(t) = -L\frac{d}{dt}iCr(t)$:

$$vLr(t) = (vCr_{max} - vO_{min} - m(vO_{min} + VD1) - VD2) \cdot cos(w_{res}t) = \frac{\Delta vLr}{2} \cdot cos(w_{res}t) \tag{57}$$

What is important is the peak voltage $\Delta vLr > 0V$ which at the end of the half resonance will add positively to vD3(t):

$$vD3_{max} = VD1 - VD2 + \frac{\Delta vLr}{2} = VD1 - 2VD2 + vCr_{max} - vO_{min} - m(vO_{min} + VD1)$$

$$= VD1 - 2VD2 + VCr + \frac{\Delta vCr}{2} - vO_{min} - m(vO_{min} + VD1) \tag{58}$$

with $\mathrm{v0_{min}} = \mathrm{VO} - \frac{\Delta \mathrm{vo_{cer}}}{2}$.

It must be

$$vD3_{max} < VD3$$

from which

$$\frac{\Delta vCr}{2} = \frac{\alpha \cdot ILm \cdot D \cdot T}{2Cr} < VD3 - VD1 + 2VD2 - VCr + vO_{min} + m(vO_{min} + VD1)$$

$$Cr > \frac{\alpha \cdot ILm \cdot D \cdot T}{2(VD3 - VD1 + 2VD2 - VCr + vO_{min} + m(vO_{min} + VD1))} \tag{59}$$

Notice that by increasing Co and thus $\mathrm{v0_{min}}$ the minimum Cr lowers. Evaluating (59) with $\mathrm{D} = \mathrm{D_{max}}$ gives

$$\frac{\Delta vCr}{2} < -0.23V$$

$$Cr > -6.41\mu F$$

This means that for the given VD1, VD2, VD3 the half resonance will always bias D3 at a certain point, independently on the chosen Cr. There are two solutions: 1) use active switch S3 to block negative voltage; 2a) decrease VD1 by using two parallel diodes for D1 or 2b) increase VD2, VD3 by using two series diodes for D2 and D3.

Apparently 2) looks like a patch-up but, while 2a) is not convenient because of low reduction in D1 forward voltage for the range $\frac{\mathrm{ID1}}{2} \rightarrow \mathrm{ID1}$, 2b) adds little power dissipation because of the small average current flowing in D2, D3. On the other hand, 1) will for sure guarantee the correct behavior of the converter using one added switch instead of two added diodes at the expense of complicating the switching control.

Both 1) and 2) will be tested. Since 1) doesn't imply any requirement on Cr, 2b) will be used for its design, hypothesizing two ZHCS400 in place of D2 and D3: later, if not reliable, this method can be dropped in favor of 1). In principle, all the analysis starting from (45) should be repeated with the updated $\mathrm{VD2} = \mathrm{VD3} = 0.5\mathrm{V}$ but, since D would change from $\mathrm{D_{r_{max}}} = 0.3853$ to $\mathrm{D_{r_{max}}} = 0.3871$, it's useless to do so since it is considered $\mathrm{D_{r_{max}}} \approx 0.39$ from [6]. Jumping then to (59), the required Cr to avoid D3 bias during Toff becomes

$$Cr > 5.64\mu F$$

It is chosen

$$Cr = 6.8\mu F \quad [11]$$

Resonant inductor Lr

Now that T_{res}, Co and Cr are known, Lr is obtained from (48) as

$$Lr = \left(\frac{T_{res}}{2\pi}\right)^2 \frac{Co+Cr(1+m)^2}{Co\ Cr} \quad (60)$$

With $\frac{T_{res}}{2} = 8.71\mu s$, $Co = Co_{cer} = 200\mu F$, $Cr = 6.8\mu F$

$$Lr = 3.02\mu H \approx 3\mu H \quad [12]$$

Input capacitor Cg

The only remaining component to be designed is the input capacitor Cg. Since it will be electrolytic to sustain $VG_{max} = 50V$, what matters is its ESR, low enough to filter all the pulsing current going through S1. A typical input capacitance can be chosen as

$$Cg = 100\mu F \quad [13]$$

Theorical numerical stresses

To sum up, all designed components and relative stresses are reported in Table 3 (S3 included). Stresses have been evaluated according to formulas of chapter IV except for $vD3_{rev}$ (and $vDS3 = -vD3_{rev}$ if D3 accidentally biases during Toff) which includes now diodes' forward drop according to (58). In order to get maximum stresses $RL = 0.5\Omega$ is used and both $VG = 46V$ and $VG = 50V$ are considered; starred values result from $VG = 50V$.

	$\mathbf{i_{rms}[A]}$	$\mathbf{v_{work}[V]}$	
$\mathbf{Cr = 6.8\mu F}$	0.45	17	
$\mathbf{Cg = 100\mu F}$	0.26	50*	
$\mathbf{Co = 200\mu F}$	2.89	2	
		$\mathbf{i_{max}[A]}$	
$\mathbf{Lr = 3\mu H}$	0.30	0.54	
$\mathbf{Lm = 25\mu H}$	4.65, 0.45	4.25*	
			$\mathbf{v_{ds}[V]}$
S1	0.34	0.61*	48*
S2	0.30	0.54	48*
S3	0.34	0.61*	0→0.65
	I [A]		$\mathbf{v_{rev}[V]}$
D1 (VD1 = 0.4V)	3.61*	7	-6.47*
D2 (VD2 = 0.5V)	0.21	0.54	-6.47*
D3 (VD3 = 0.5V)	0.21	0.61*	-0.65

Table 3

Expected efficiency

At this point, the efficiency can be evaluated:

$$\eta = \frac{IO\ VO}{IG\ VG} = \frac{IO}{IG} M$$

One may be tempted to say that η_{max} occurs for M_{max} forgetting that when VG = 46V IG increases as well while IO remains constant. Turns out that, for all considered loads, little changes:

$$\eta_{46V} = 0.8297 \approx 0.83$$

$$\eta_{50V} = 0.83$$

The converter can't reach a better efficiency since diodes' forward voltage is taken in account but other sources off loss are not (switches, copper losses, etc.). Even so, looking at Tab. 3, it's clear that D1 is a non-negligible cause of power loss w.r.t. the power level treated by the converter, dissipating $P_{D1} = ID1 \cdot VD1 \approx 1.4W$ when PO = 8W. If VD1 cannot be reduced, an active switch S4 may be used in place of D1; a STN3NF06L satisfies stresses with $r_{on} \approx 70m\Omega$ @ IS1 = ID1 ≈ 3.6A: since $iD1_{rms} \approx iPrim_{rms}$ it dissipates the average power

$$P_{S4} \approx iPrim_{rms}^2 \cdot r_{on} = 4.65^2 \cdot 0.07W = 1.51W$$

which is slightly more than what D1 dissipates. A switch with $r_{on} < 70m\Omega$ should be chosen to replace D1.

Regarding the switching losses, S2 ideally switches on and off both at ZCS, its current being the discussed half resonance. Moreover, it can be switched on at ZVS if the command that turns S1 off and which is inverted and forwarded to S2 is delayed: the current flowing in L starts discharging the parasitic C_{ds} of S2 and eventually biases its body diode. Similarly, is off-phase resonance is prematurely interrupted, the current flowing in Lr can bias the body diode of S1 to let it turn on at ZVS; its turn off is hard-switched anyways.

VI SIMULATIONS

In order to verify the behavior of the circuit and the correctness of the found analytical formulas, simulations have been run through PLECS software. The Ćuk-Buck 1.5 schematic is shown in Fig. 29.

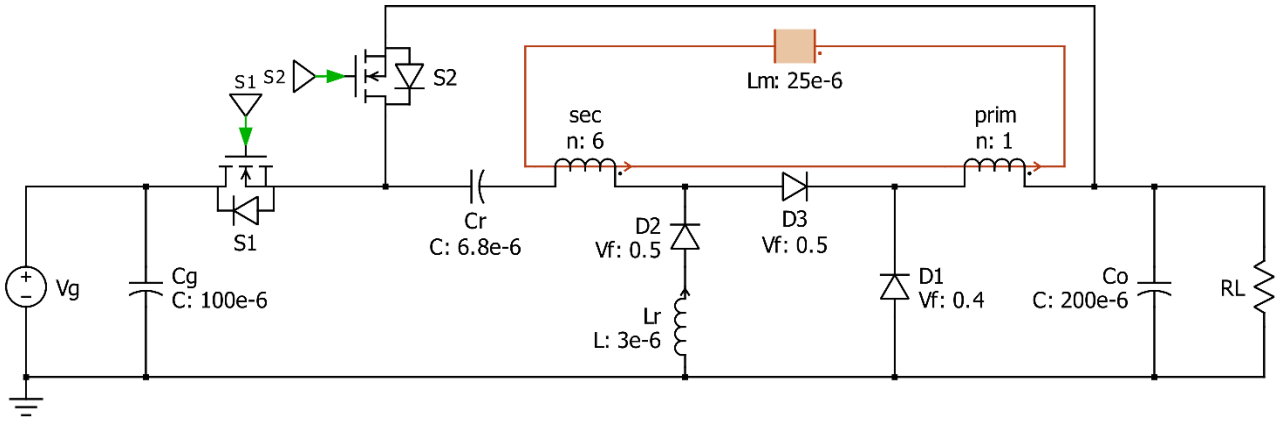

Figure 29

For all following simulations voltages/currents will be in blue/red; continuous/dotted lines mean heavy/light load condition.

VG = 46V, light and heavy load

The first simulation is for VG = 46V and IO = 4, 1A. Fig. 30 shows vCr, iCr, iLr at cycle-stationary condition of the converter. As S1 goes on the input current, approximately constant around $\alpha \cdot$ ILm, charges Cr and vCr ramps up practically linearly. Once Ton ends S1 opens and S2 closes: Lr-Cr resonance starts and Cr is discharged of Q_g. Notice that the half resonance duration coincides, if not for a negligible time interval, with the designed Toff, meaning that (48) is a good approximation of the resonance period.

Fig. 31 displays vo, io, iLm. Looking at iLm it's clear that most of the dc output current comes from ILm: as see in chapter II, Ćuk-Buck 2 and then Ćuk-Buck 1.5 are evolutions of the tapped-inductor Buck converter with the magnetic leakage management more and more refined.

Figure 30

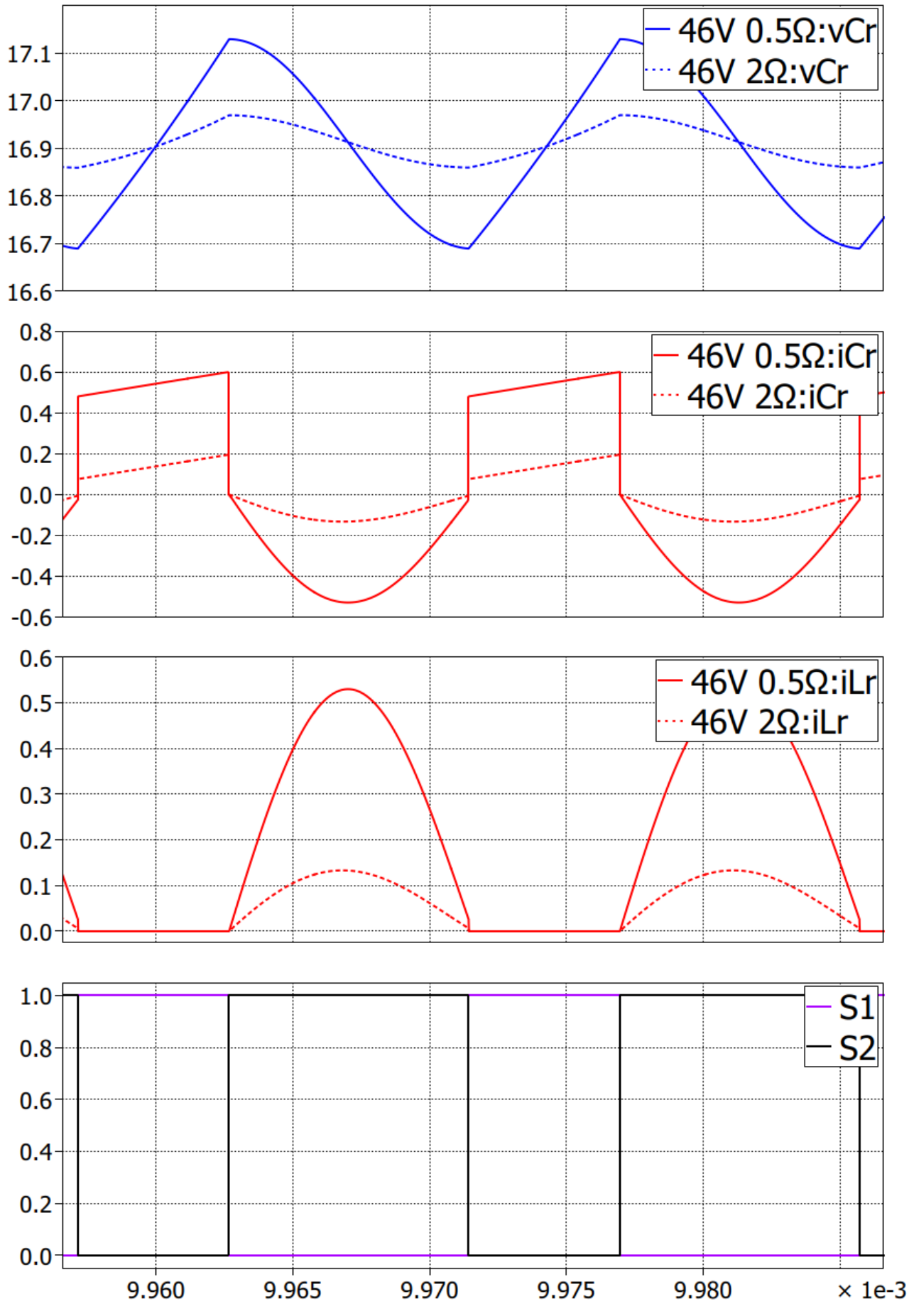
46V 0.5Ω:vCr
46V 2Ω:vCr
17.1
17.0
16.9
16.8
16.7
16.6
46V 0.5Ω:iCr
46V 2Ω:iCr
0.8
0.6
0.4
0.2
0.0
-0.2
-0.4
-0.6
46V 0.5Ω:iLr
46V 2Ω:iLr
0.6
0.5
0.4
0.3
0.2
0.1
0.0
S1
S2
1.0
0.8
0.6
0.4
0.2
0.0
9.960
9.965
9.970
9.975
9.980
× 1e-3

Figure 31

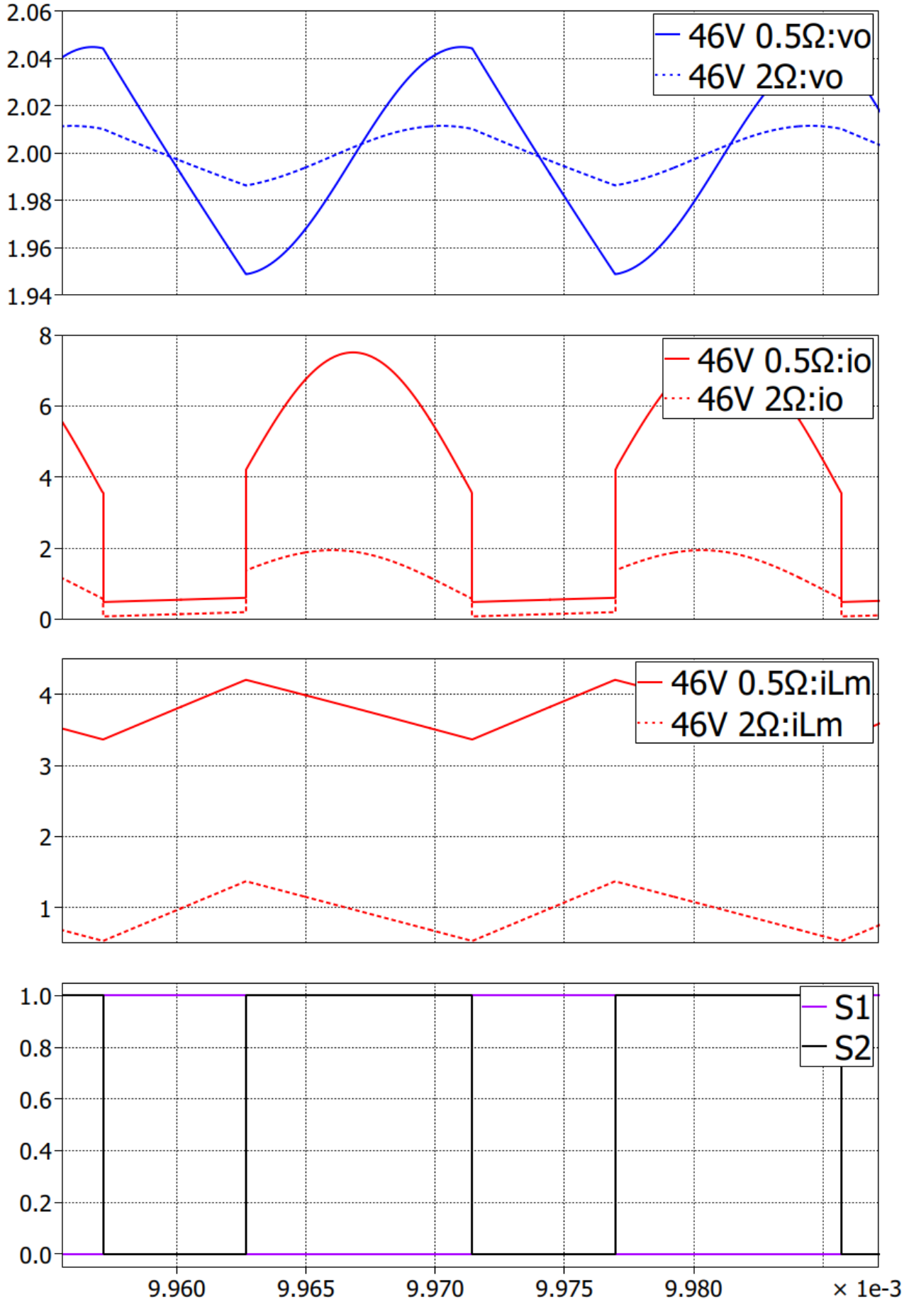
2.06
2.04
2.02
2.00
1.98
1.96
1.94
46V 0.5Ω:vo
46V 2Ω:vo
8
6
4
2
0
46V 0.5Ω:io
46V 2Ω:io
4
3
2
1
46V 0.5Ω:iLm
46V 2Ω:iLm
1.0
0.8
0.6
0.4
0.2
0.0
S1
S2
9.960
9.965
9.970
9.975
9.980
× 1e-3

It is interesting to look at the discussed vD3(t) during Toff: as designed, D3 remains unbiased but S3 may be used to give better robustness to the real converter.

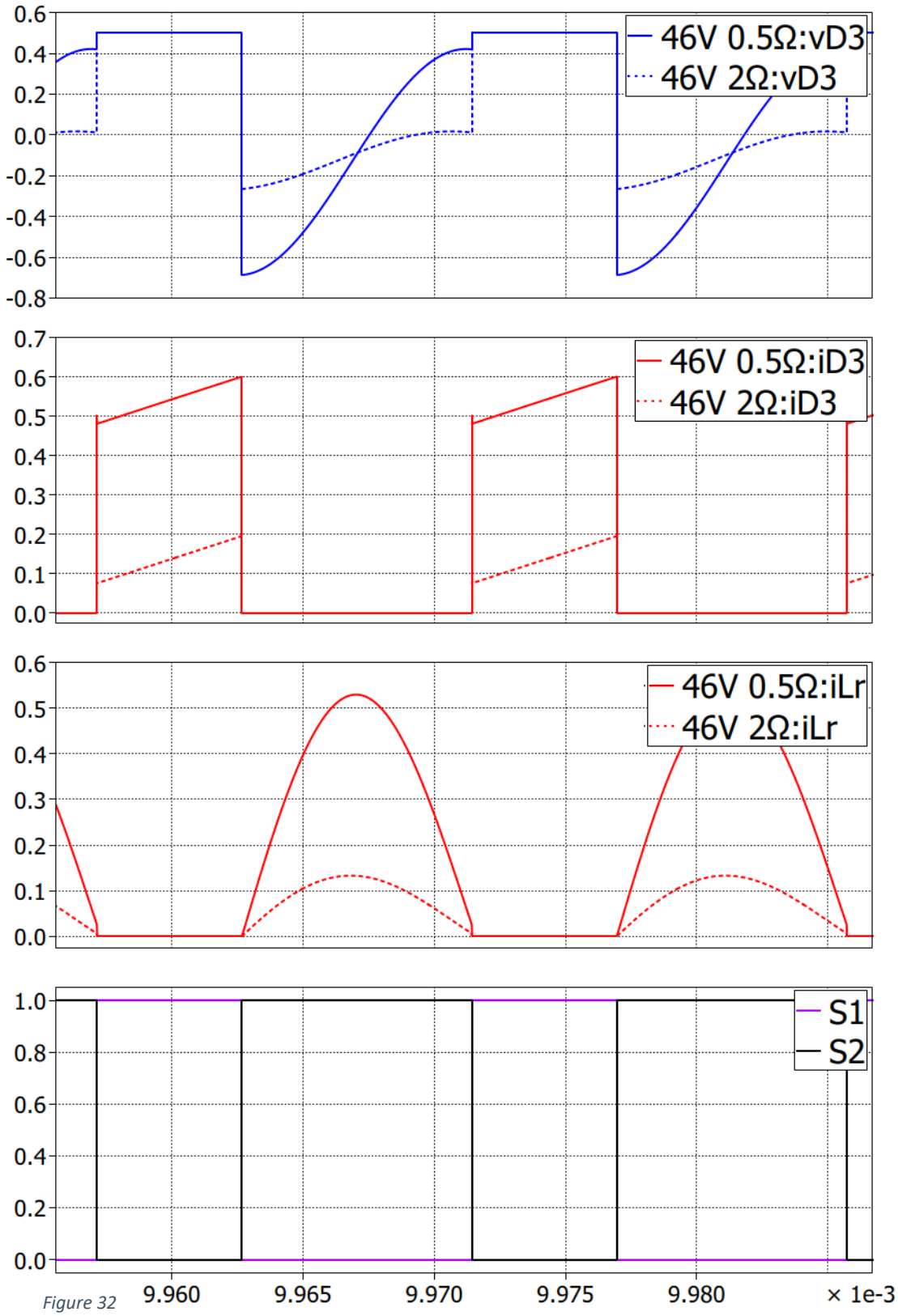

Figure 32

VG = 50V, light and heavy load

The same waveforms are shown for VG = 50V.

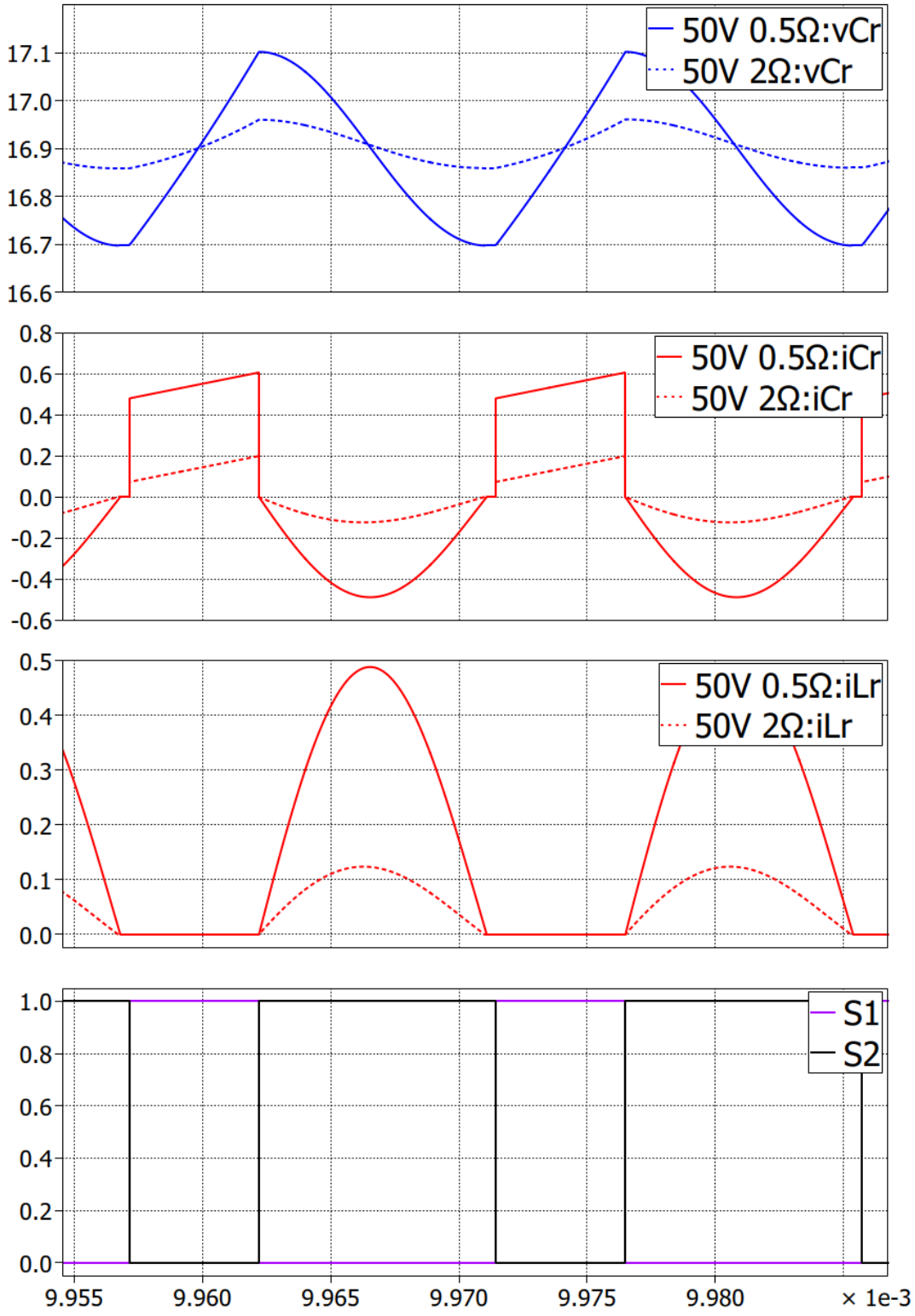

Figure 33

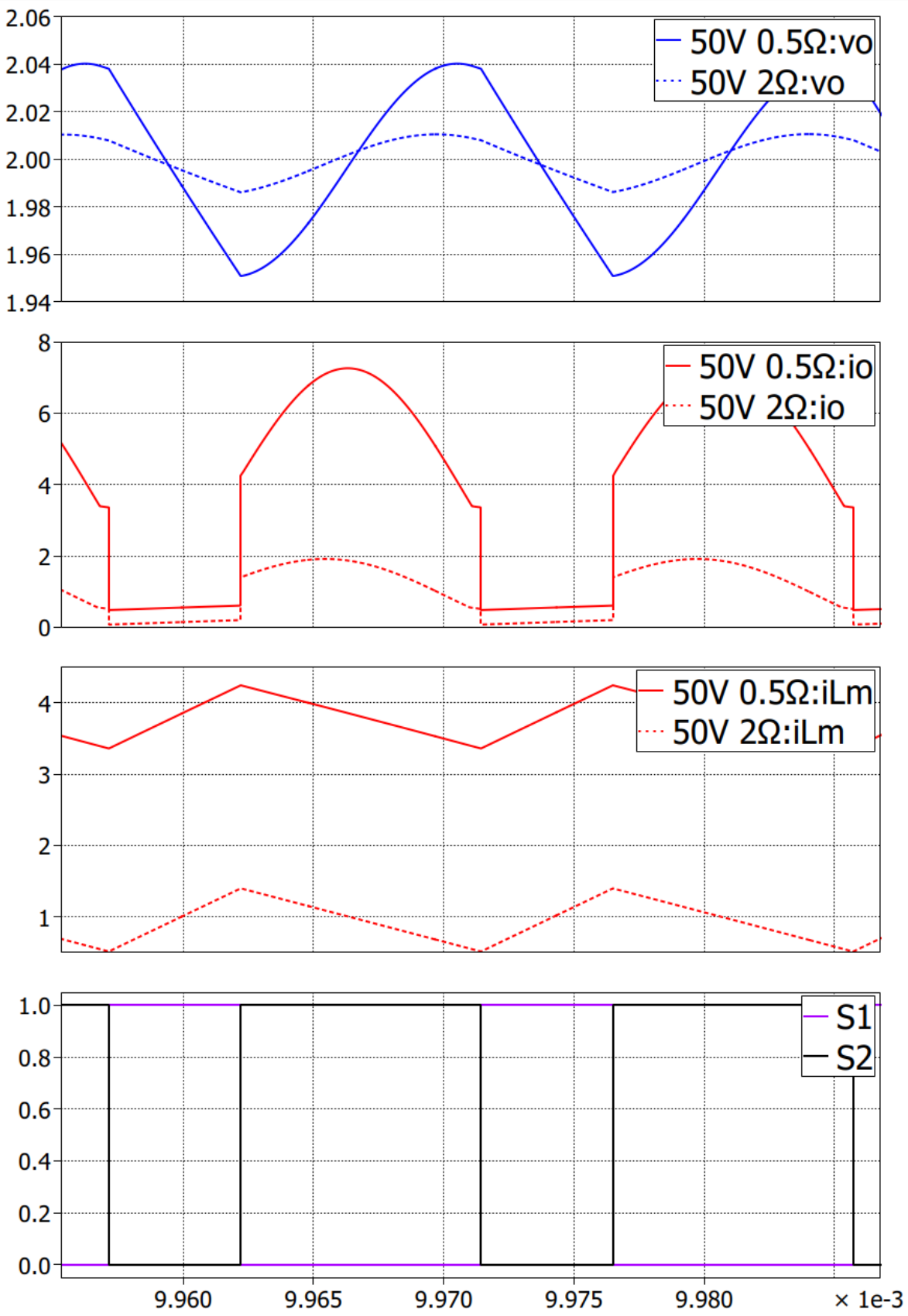
2.06
2.04
2.02
2.00
1.98
1.96
1.94
50V 0.5Ω:vo
50V 2Ω:vo
8
6
4
2
0
50V 0.5Ω:io
50V 2Ω:io
4
3
2
1
50V 0.5Ω:iLm
50V 2Ω:iLm
1.0
0.8
0.6
0.4
0.2
0.0
S1
S2
9.960
9.965
9.970
9.975
9.980
× 1e-3

Figure 34

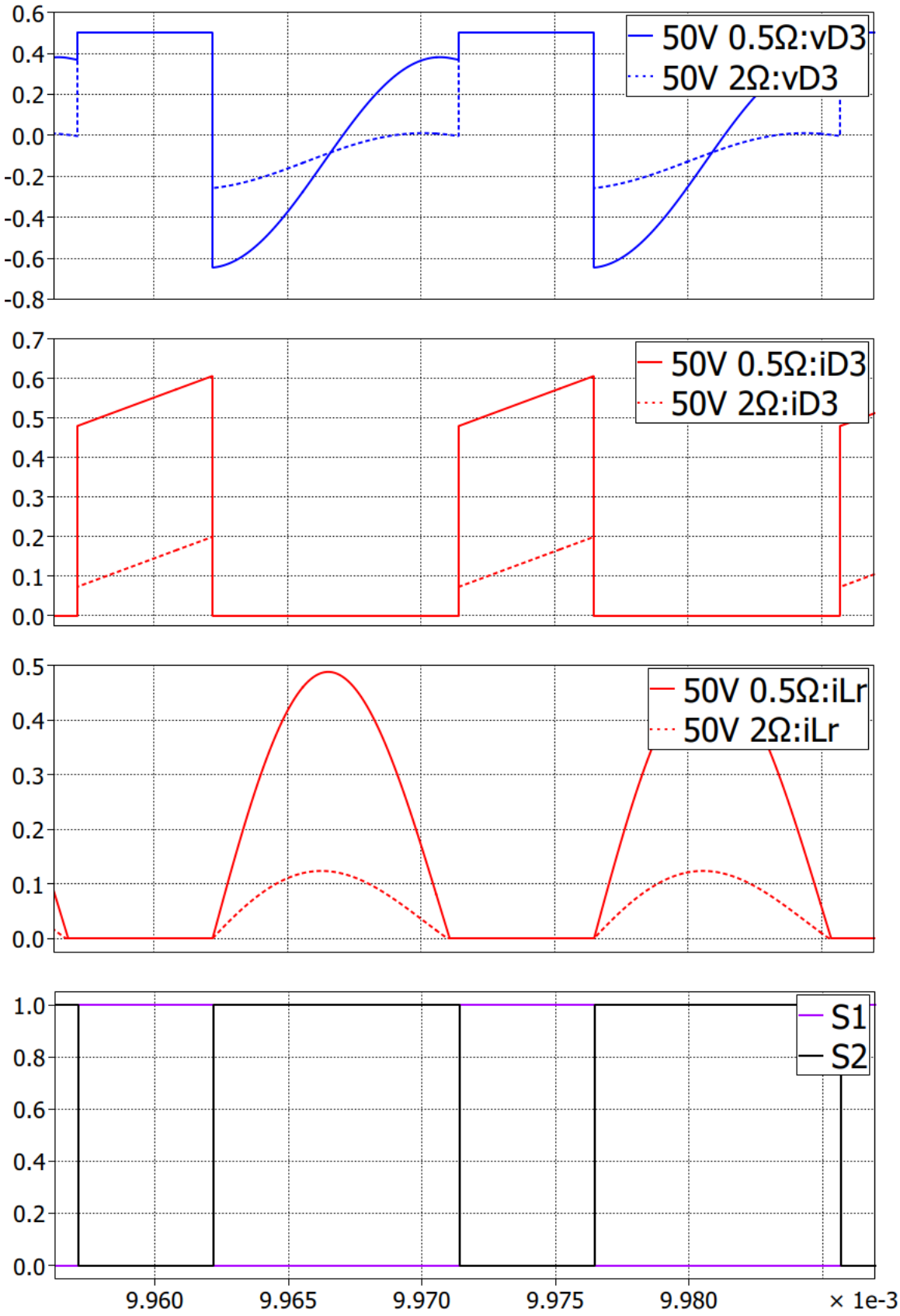
0.6
0.4
0.2
0.0
-0.2
-0.4
-0.6
-0.8
50V 0.5Ω:vD3
50V 2Ω:vD3
0.7
0.6
0.5
0.4
0.3
0.2
0.1
0.0
50V 0.5Ω:iD3
50V 2Ω:iD3
0.5
0.4
0.3
0.2
0.1
0.0
50V 0.5Ω:iLr
50V 2Ω:iLr
1.0
0.8
0.6
0.4
0.2
0.0
S1
S2
9.960
9.965
9.970
9.975
9.980
× 1e-3

Figure 35

As expected, since $D = D_{min}$ due to $VG = 50V = VG_{max}$, Toff increases allowing more time for the Lr-Cr half resonance which is stopped by D2 anyways.

Simulated numerical stresses

Exploiting PLECS automatic average, rms and maximum measurements of the plotted waveforms, worst case stresses are obtained in Tab. 4 which can be confronted with the theorical ones in Tab. 3 (chapter V).

	$\mathbf{i_{rms}[A]}$	$\mathbf{v_{work}[V]}$	
$\mathbf{Cr = 6.8\mu F}$	0.45	17	
$\mathbf{Cg = 100\mu F}$	0.26[4]	50*	
$\mathbf{Co = 200\mu F}$	2.89	2	
		$\mathbf{i_{max}[A]}$	
$\mathbf{Lr = 3\mu H}$	0.29	0.53	
$\mathbf{Lm = 25\mu H}$	4.64, 0.45	4.24*	
			$\mathbf{v_{ds}[V]}$
S1	0.34	0.61*	48*
S2	0.29	0.53	48*
S3	0.34	0.61*	0
	I [A]		$\mathbf{v_{rev}[V]}$
D1 (VD1 = 0.4V)	3.61*	6.98	-6.43*
D2 (VD2 = 0.5V)	0.21	0.53	-6.93*
D3 (VD3 = 0.5V)	0.21	0.61*	-0.69

Table 4

Notice that vD2 accounts here for D3 forward drop $VD3 = 0.5V$, that's why it differs of about half Volt from the theorical value in Tab. 3.

Since simulated stresses are almost identical to the theorical ones, the correctness of chapter IV expressions is verified.

[4] The input capacitor current has been obtained through a dedicated simulation hypothesizing an equivalent source resistance $Rg = 5\Omega$.

Leakages management

Until now no delay is present between on and off-phase (T2 = 0s) in agreement with what has been highlighted in chapter III. In order to demonstrate the main purpose of the Ćuk-Buck 1.5 converter, a leakage inductance Llk_s is added at the secondary side of the coupled-inductors model so that a direct comparison with the Ćuk-Buck 2 can be done: in the original converter it was Lr which, even in a leakage-free scenario, ended up in series with Cr.

In order to pick Llk_s, the effect of coupling coefficient k = 0.99 is first analyzed. Supposing symmetrical primary and secondary leakages $Llk = Llk_s = Llk_p$ it is:

$$Llk = \frac{-k(1+m^2)+\sqrt{4m^2+k^2(m^2-1)^2}}{2k} Lm = 0.02Lm = 0.5\mu F$$

Figure 36 shows the schematic with Llk_s included:

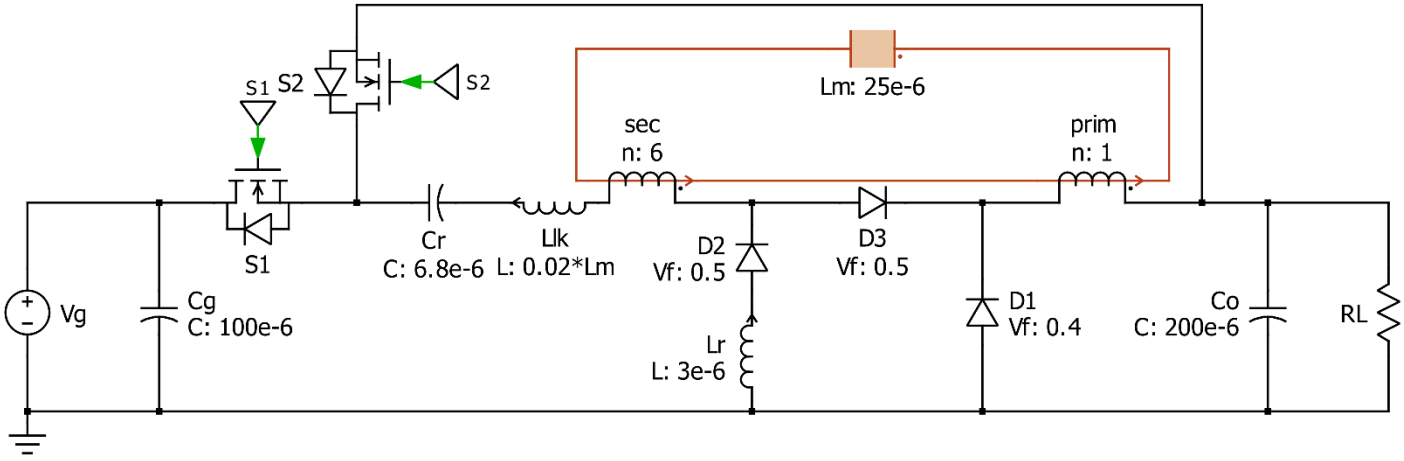

Figure 36

The resonance period becomes

$$T_{off\,min\,new} = \frac{T_{res\,new}}{2} = \pi\sqrt{(Lr+Llk)Cr}\cdot\sqrt{\frac{Co}{Co+Cr(1+m)^2}} = 9.41\mu s > 8.71\mu s = T_{off\,\min} \quad (61)$$

with $T_{off_{min}}$ being the previously design off-phase duration.

As expected, the Lr-Cr resonance doesn't complete as shown in Fig. 37 where $VG = 46,50V$ is being tested ($V = 50V \rightarrow D = D_{max}$ in dotted lines).

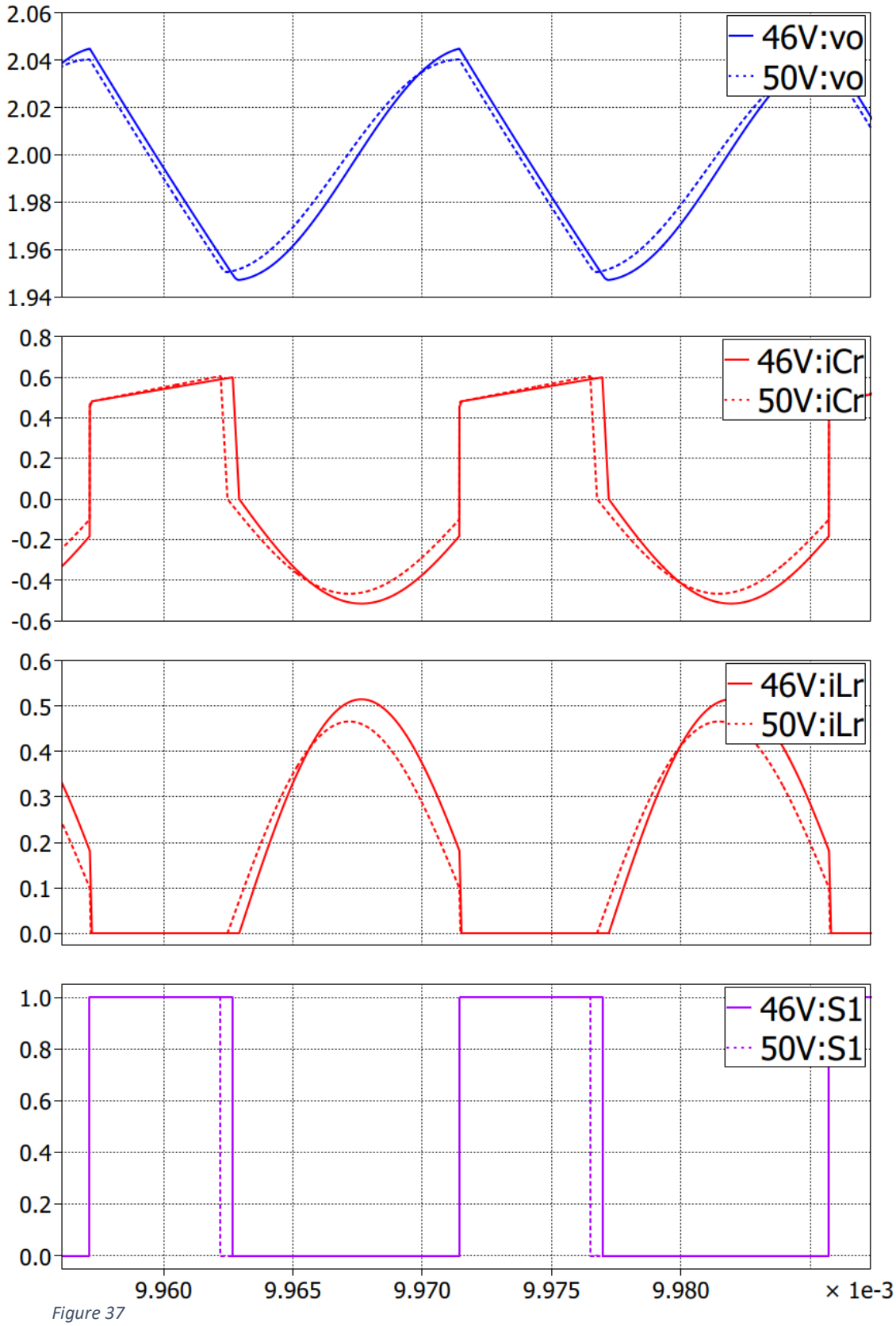
2.06
2.04
2.02
2.00
1.98
1.96
1.94
46V:vo
50V:vo
0.8
0.6
0.4
0.2
0.0
-0.2
-0.4
-0.6
46V:iCr
50V:iCr
0.6
0.5
0.4
0.3
0.2
0.1
0.0
46V:iLr
50V:iLr
1.0
0.8
0.6
0.4
0.2
0.0
46V:S1
50V:S1
9.960
9.965
9.970
9.975
9.980
× 1e-3

Figure 37

Still, as explained in III, the transition between on and off-phase is very fast, iCr dropping to 0A almost instantaneously right after $t = DT$.

In this case, because of the short cut-off of the half resonance, the output voltage is not affected but in general worse coupling factors ($k \approx 0.9$) must be taken in account. The design can fix $T_{off_{min}}$ for the expected worst-case coupling i.e. for the largest leakage inductance so that D_{max} is capable of ensure the half resonance to always complete.

APPENDIX A: time description of the Ćuk-Buck 1.5

First, constant VO (infinite Co) is assumed during T_{on} and T_{off}.

ON-PHASE: $0 \leq t < DT$

$$\begin{cases} iCr(t) = Cr\frac{d}{dt}vCr(t) \\ vCr(t) = VG - VO - vL(t) \\ vL(t) = L\frac{d}{dt}iCr(t) \end{cases}$$

Initial conditions on state variables:

$$\begin{cases} vCr(0) = vCr_{min} \\ iL(0) = iCr(0^+) = iL_{min} \end{cases}$$

with $iL_{min} = \alpha \cdot iLm_{min}$. Variable of interests are vCr(t), iCr(t) = iL(t) = io(t):

$$vCr(t) = VG - VO + (vC_{min} - VG + VO)Cos\left(\frac{t}{\sqrt{L\,Cr}}\right) + iL_{min}\sqrt{\frac{L}{Cr}}Sin\left(\frac{t}{\sqrt{L\,Cr}}\right)$$

$$iCr(t) = -(vC_{min} - VG + VO)\sqrt{\frac{Cr}{L}}Sin\left(\frac{t}{\sqrt{L\,Cr}}\right) + iL_{min}Cos\left(\frac{t}{\sqrt{L\,Cr}}\right)$$

Since $L = \frac{(N1+N2)^2}{N1^2}Lm \approx 50Lm \gg Lr$, $w_{res_{on}} = \frac{1}{\sqrt{L\,Cr}} \ll \frac{1}{\sqrt{Lr\,Cr}}$ and thus the cosine and sine terms can be approximated with their first order Taylor expansion:

$$vCr(t) \approx VG - VO + (vC_{min} - VG + VO) + \frac{iL_{min}}{Cr}t = vC_{min} + \frac{iL_{min}}{Cr}t \qquad (A1)$$

$$iCr(t) \approx iL_{min} + \frac{VG - vC_{min} - VO}{L}t \qquad (A2)$$

(A1), (A2) translates in the linear approximation made for the on-phase: Cr is charged at constant current iLm_{min} while constant voltage $vC_{min} - VG + VO$ drops on L, building it's flux linearly in time.

OFF-PHASE: DT $\leq$ t < T

$$\begin{cases} iCr(t) = Cr\frac{d}{dt}vCr(t) \\ vCr(t) = (m+1)VO + vLr(t) \\ vLr(t) = -Lr\frac{d}{dt}iCr(t) \end{cases}$$

$$vLm(t) = -VO = Lm\frac{d}{dt}iLm(t)$$

Initial conditions on state variables:

$$\begin{cases} vCr(DT) = vCr_{max} \\ iLr(DT) = -iCr(DT^{+}) = 0A \end{cases}$$

$$iLm(DT) = \frac{iCr(DT^{-})}{\alpha} = iLm_{max}$$

Variable of interests are vCr(t), iCr(t), iLm(t):

$$vCr(t) = (1+m)VO + (vC_{max} - (1+m)VO)Sin\left(\frac{t}{\sqrt{L\,Cr}}\right)$$

$$iCr(t) = -((1+m)VO - vC_{max})\sqrt{\frac{Cr}{Lr}}Cos\left(\frac{t}{\sqrt{L\,Cr}}\right)$$

$$iLm(t) = iLm_{max} - \frac{VO}{Lm}t$$

In the following, the model is refined considering the effect of finite Co.

ON-PHASE (Co $\neq \infty$): 0 $\leq$ t < DT

$$\begin{cases} iCr(t) = Cr\frac{d}{dt}vCr(t) \\ vCr(t) = VG - vo(t) - vL(t) \\ vL(t) = L\frac{d}{dt}iCr(t) \\ iCr(t) = Co\frac{d}{dt}vo(t) \end{cases}$$

Initial conditions on state variables:

$$\begin{cases} vCr(0) = vCr_{min} \\ iL(0) = iCr(0^{+}) = iL_{min} \\ vo(0) = vo_{min} \end{cases}$$

Variable of interests are vo(t), vCr(t), iCr(t) = iL(t) = io(t):

$$vo(t) = \frac{(Cr\,VG + Co\,vo_{min} - Cr\,vCr_{min}) + Cr(vCr_{min} + vo_{min} - VG)Cos\left(\sqrt{\frac{Co+Cr}{L\,CoCr}}\,t\right)}{Co+Cr} + iL_{min}\sqrt{\frac{L\,Cr}{Co(Co+Cr)}}\,Sin\left(\sqrt{\frac{Co+Cr}{L\,CoCr}}\,t\right) \qquad \text{(A3)}$$

$$iCr(t) = Co\frac{d}{dt}vo(t) = \frac{-CoCr(vCr_{min} + vo_{min} - VG)\sqrt{\frac{Co+Cr}{L\,CoCr}}\,Sin\left(\sqrt{\frac{Co+Cr}{L\,CoCr}}\,t\right)}{Co+Cr} + iL_{min}Cos\left(\sqrt{\frac{Co+Cr}{L\,CoCr}}\,t\right) =$$

$$= -(vCr_{min} + vo_{min} - VG)\sqrt{\frac{Co\,Cr}{L\,(Co+Cr)}}\,Sin\left(\sqrt{\frac{Co+Cr}{L\,CoCr}}\,t\right) + iL_{min}Cos\left(\sqrt{\frac{Co+Cr}{L\,CoCr}}\,t\right) \qquad \text{(A4)}$$

$$vL(t) = L\frac{d}{dt}iCr(t) = -L(vCr_{min} + vo_{min} - VG)\frac{1}{L}Cos\left(\sqrt{\frac{Co+Cr}{L\,CoCr}}\,t\right) - L\,iL_{min}\sqrt{\frac{Co+Cr}{L\,CoCr}}\,Sin\left(\sqrt{\frac{Co+Cr}{L\,CoCr}}\,t\right) =$$

$$= -(vCr_{min} + vo_{min} - VG)Cos\left(\sqrt{\frac{Co+Cr}{L\,CoCr}}\,t\right) - iL_{min}\sqrt{\frac{L(Co+Cr)}{CoCr}}\,Sin\left(\sqrt{\frac{Co+Cr}{L\,CoCr}}\,t\right) \qquad \text{(A5)}$$

$$vCr(t) = VG - vo(t) - vL(t) =$$

$$= VG - \frac{(Cr\,VG + Co\,vo_{min} - Cr\,vCr_{min}) + Cr(vCr_{min} + vo_{min} - VG)Cos\left(\sqrt{\frac{Co+Cr}{L\,CoCr}}\,t\right)}{Co+Cr} - iL_{min}\sqrt{\frac{L\,Cr}{Co(Co+Cr)}}\,Sin\left(\sqrt{\frac{Co+Cr}{L\,CoCr}}\,t\right) +$$

$$+(vCr_{min} + vo_{min} - VG)Cos\left(\sqrt{\frac{Co+Cr}{L\,CoCr}}\,t\right) + iL_{min}\sqrt{\frac{L(Co+Cr)}{CoCr}}\,Sin\left(\sqrt{\frac{Co+Cr}{L\,CoCr}}\,t\right) =$$

$$= \frac{Co}{Co+Cr}VG + \frac{Cr\,vCr_{min} - Co\,vo_{min}}{Co+Cr} + \frac{-Cr(vCr_{min} + vo_{min} - VG) + (vCr_{min} + vo_{min} - VG)(Co+Cr)}{Co+Cr}Cos\left(\sqrt{\frac{Co+Cr}{L\,CoCr}}\,t\right) +$$

$$+iL_{\min}\left(\sqrt{\frac{L(Co+Cr)}{CoCr}} - \sqrt{\frac{L\,Cr}{Co(Co+Cr)}}\right)Sin\left(\sqrt{\frac{Co+Cr}{L\,CoCr}}\,t\right) =$$

$$= \frac{Co}{Co+Cr}VG + \frac{Cr\,vCr_{min} - Co\,vo_{min}}{Co+Cr} + \frac{(vCr_{min} + vo_{min} - VG)Co}{Co+Cr}Cos\left(\sqrt{\frac{Co+Cr}{L\,CoCr}}\,t\right) + iL_{\min}\sqrt{\frac{L\,Co}{Cr(Cr+Co)}}\,Sin\left(\sqrt{\frac{Co+Cr}{L\,CoCr}}\,t\right) \qquad \text{(A6)}$$

In order to verify these expressions, they should become similar to those with infinite Co once it is considered that $\mathrm{Co} = 200\mu\mathrm{F} \gg \mathrm{Cr} = 6.8\mu\mathrm{F}$. In this case $\frac{\mathrm{Co}}{\mathrm{Co+Cr}} \approx \mathrm{Co}$, $\frac{\mathrm{Co+Cr}}{\mathrm{CoCr}} \approx \frac{1}{\mathrm{Cr}}$ are valid approximations and vo(t), iCr(t), vCr(t) become:

$$vo(t) \approx \frac{(Cr\,VG + Co\,vo_{min} - Cr\,vCr_{min}) + Cr(vCr_{min} + vo_{min} - VG)Cos\left(\frac{1}{\sqrt{L\,Cr}}t\right)}{Co} + iL_{min}\frac{\sqrt{L\,Cr}}{Co}Sin\left(\frac{1}{\sqrt{L\,Cr}}t\right)$$

$$iCr(t) \approx -(vCr_{min} + vo_{min} - VG)\sqrt{\frac{Cr}{L}}\,Sin\left(\frac{1}{\sqrt{L\,Cr}}t\right) + iL_{min}Cos\left(\frac{1}{\sqrt{L\,Cr}}t\right)$$

$$vCr(t) \approx VG + \frac{Cr\ vCr_{min} - Co\ vo_{min}}{Co} + \frac{(vCr_{min} + vo_{min} - VG)Co}{Co} Cos\left(\frac{1}{\sqrt{L\ Cr}}t\right) + iL_{\min}\sqrt{\frac{L}{Cr}}\, Sin\left(\frac{1}{\sqrt{L\ Cr}}t\right)$$

Then, since $\frac{1}{\sqrt{\mathrm{L\ Cr}}} \ll \frac{1}{\sqrt{\mathrm{Lr\ Cr}}}$, vo(t), iCr(t), vCr(t) can be approximated with their first order Taylor expansion:

$$vo(t) \approx \frac{vo_{min}(Co+Cr)}{Co} - \frac{iL_{min}}{Co}t \approx vo_{min} + \frac{iL_{min}}{Co}t \quad \text{(A7)}$$

$$iCr(t) \approx \frac{VG - vCr_{min} - vo_{min}}{L}t + iL_{min} \quad \text{(A8)}$$

$$vCr(t) \approx \frac{vCr_{min}(Co+Cr)}{Co} - \frac{iL_{\min}}{Cr}t \approx vCr_{min} + \frac{iL_{\min}}{Cr}t \quad \text{(A9)}$$

(A3) tells that the output capacitor is being charged with constant current $iL_{\min}$: this would be true if no load is present which in reality draws some of the slow resonant current. Since A8/A9 coincide with A2/A1 (if not for $VO \neq vo_{\min}$ since the output voltage is now a state variable) the expressions A3→6 are verified.

OFF-PHASE ($Co \neq \infty$): $DT \leq t < T$

$$\begin{cases} iCr(t) = Cr\frac{d}{dt}vCr(t) \\ vCr(t) = (1+m)vo(t) + vLr(t) \\ vLr(t) = -Lr\frac{d}{dt}iCr(t) \\ -(1+m)iCr(t) + iLm(t) = Co\frac{d}{dt}vo(t) \\ -vo(t) = Lm\frac{d}{dt}iLm(t) \end{cases}$$

Initial conditions on state variables:

$$\begin{cases} vCr(DT) = vCr_{max} \\ iLr(DT) = -iCr(DT^{+}) = 0A \\ vo(DT) = vo_{min} \\ iLm(DT) = \frac{iCr(DT^{-})}{\alpha} = iLm_{max} \end{cases}$$

Unfortunately, the author is not able to get a solution of the system. Not considering iLm(t) (and R) makes it possible but, since the expressions would be quite approximate, only iCr(t) is reported, whose resonance frequency is used for the design of the converter:

$$iCr(t) \approx \sqrt{\frac{Co}{Co+Cr(1+m)^2}}\sqrt{\frac{Cr}{Lr}}((1+m)vo_{min} - vC_{max})Sin\left(\sqrt{\frac{Co+Cr(1+m)^2}{Co}}\frac{1}{\sqrt{Lr\ Cr}}t\right) \quad \text{(A10)}$$

APPENDIX B: conversion ratio inclusive of diodes' forward voltage

The average voltage on Lm during on/off-phase is

$$VLm_{on} = (VG - VCr - VO - VD3)\frac{N1}{N1+N2}$$

$$VLm_{off} = -(VO + VD1)$$

with

$$VCr = VO + VD2 + m(VO + VD1)$$

Flux balance on Lm brings

$$VLm_{on}D + VLm_{off}(1 - D) = 0V$$

$$(VG - (VO + VD2 + m(VO + VD1)) - VO - VD3)\frac{N1}{N1+N2}D = (VO + VD1)(1 - D)$$

from which

$$VO\left(1 - D + \frac{N1}{N1+N2}D(2 + m)\right) = -VD1(1 - D) + \frac{N1}{N1+N2}D(-VD3 - VD2 - m\,VD1) + \frac{N1}{N1+N2}D\,VG$$

$$VO(N1 + N2 - DN2 + DN1 + m\,D\,N1) = VD1(N1 + N2)(D - 1) - D\,N1(VD3 + VD2 + mVD1) + D\,N1\,VG$$

$$VO(N1(1 + D) + N2) = VD1(N1(D - 1) - N2) - D\,N1(VD2 + VD3) + D\,N1\,VG$$

$$VO = \frac{VD1(N1(D-1)-N2)-D\,N1(VD2+VD3)}{N1(1+D)+N2} + \frac{D\,N1}{N1(1+D)+N2}VG \qquad (44)$$

BIBLIOGRAPHY

[1] K. Liu, R. Oruganti and F. C. Lee, “Resonant Switches: Topologies and Characteristics,” in Proc. IEEE Power Electron. Spec. Conf. Rec., 1985, pp. 106-116.

[2] K. M. Smith, Jr. and K. Smedley, “A Comparison of Voltage-Mode Soft Switching Methods for PWM Converters,” IEEE Trans. Power Electron., vol. 12, (no. 2), pp. 376–386, Mar. 1997.

[3] K. M. Smith, Jr. and K. Smedley, “Properties and Synthesis of Passive Lossless Soft-Switching PWM Converters,” IEEE Trans. Power Electron., vol. 14, (no. 5), pp. 890-899, Sep. 1999.

[4] A. Abramovitz, C-S. Liao and K. Smedley, “State-Plane Analysis of Regenerative Snubber for Flyback Converters,” IEEE Trans. Power Electron., vol. 28, (no. 11), pp. 5323-5332, Nov. 2013.

[5] V. Vorpérian, “Analysis of Resonant Converters”, PhD thesis, California Institute of Technology, Pasadena, California, 1984.

[6] S. Ćuk, Four-switch step-down storage less converter, U.S. Patent 8 134 315 B2, Mar. 13, 2012.

[7] H. Matsuo and K. Harada, “The Cascade Connection of Switching Regulators,” IEEE Trans. Ind. Appl., vol. IA-12, (no. 2), Mar./Apr. 1976.

[8] D. Maksimović and S. Ćuk, “Switching Conveters with Wide DC Conversion Range,” IEEE Trans. Power Electron., vol. 6, (no. 1), Jan. 1991.

[9] Ankit Chadha, Agasthya Ayachit, Dalvir K. Saini, and Marian K. Kazimierczuk, “Steady-State Analysis of PWM Tapped-Inductor Buck DC-DC Converter in CCM”, 2018 IEEE Texas Power and Energy Conference (TPEC).

[10] S. Ćuk, Hybrid-switching step-down converter with a hybrid transfomer, U.S. Patent 9 231 471 B2, Jan. 5, 2016.